

1 Breakage, scarring, scratches and explosions: understanding impact 2 trace formation on quartz

3
4 Noora Taipale
5 TraceoLab / Prehistory, University of Liège
6 Quai Roosevelt 1 B (Bât. A4)
7 4000 Liège
8 Belgium
9 noora.taipale@uliege.be
10 +32 (0)479 44 85 98

11
12 Veerle Rots
13 TraceoLab / Prehistory, University of Liège
14 Chercheure qualifiée du FNRS
15 Quai Roosevelt 1 B (Bât. A4)
16 4000 Liège
17 Belgium

20 Abstract

21 Quartz projectiles have received attention in the recent years due to, for instance, their discovery at
22 prominent South African Middle Stone Age sites. However, very few methodological studies have
23 been dedicated to quartz armatures and the ones published so far are not built on an understanding
24 of the particular behaviour of quartz under mechanical stress. Here we investigate impact damage
25 formation on automorphic and xenomorphic quartz (crystal quartz and vein quartz) through the
26 microscopic analysis of 91 experimental armatures using a combination of low and high
27 magnifications and SEM. Our results show that the structural properties of quartz affect the
28 attributes of impact breaks and other damage. We also examine wear patterns on three different
29 types of projectiles, and offer preliminary guidelines for identifying them in archaeological
30 assemblages. We argue that while quartz assemblages withhold significant potential for
31 understanding past hunting technologies, the methods used for identifying and interpreting quartz
32 projectiles need to be adjusted so that they take into account the notable differences between the
33 macrocrystalline and cryptocrystalline varieties of this raw material.

35 Keywords

36 quartz; projectiles; barbs; transverse points; impact damage; microwear

38 Acknowledgements

39 This research was funded by the European Research Council under the European Union's Seventh
40 Framework Programme (FP/2007–2013, ERC Grant Agreement Nr. 312283, Veerle Rots). Noora
41 Taipale is also indebted to the Kone Foundation (grant number 088817) and Veerle Rots to the Fund
42 for Scientific Research (FNRS-FRS). We would like to thank Johanna Seppä who kindly provided us
43 with her experimental material that supplemented this study and Hanna Konttinen who transported
44 the material. We are grateful to the members of TraceoLab for their support and advice, and
45 particularly want to thank Christian Lepers for his participation in the experiments, Dries Cnuts for

1 his help with the SEM imaging, and Justin Coppe for his assistance in the experiments and his
2 comments on an earlier version of this manuscript.

3 4 1 Introduction

5 Quartz is a key component in southern African MSA industries that have become important for the
6 study of the early development of hunting technologies (Lombard 2011; Rots et al. 2017; de la Peña
7 et al. 2018). Quartz projectiles have recently been reported from for example Sibudu Cave (South
8 Africa), where quartz backed elements have been interpreted as evidence of the use of bow and
9 arrow 60 Kya (Lombard 2011). Despite the increasing importance of this lithic raw material for
10 archaeological interpretations, very little methodological work has been done to understand impact
11 wear on it. Until very recently (Fernández-Marchena et al. 2017), quartz projectiles have mainly
12 been characterised using methods originally developed for flint and other cryptocrystalline rocks
13 (e.g. Pargeter 2013), and a limited amount of systematic work has been done to understand the
14 differences between quartz and flint-like rocks in in this respect. This is regardless of the fact that
15 the recent decades have seen advances in functional analysis of quartz tools and a renewed interest
16 in quartz industries in general (e.g. Knutsson 1988; Knutsson et al. 2015b; de Lombera-Hermida and
17 Rodríguez-Rellán 2016 and references therein; Márquez et al. 2016; Ollé et al. 2016).

18 Both automorphic (crystal) and xenomorphic (vein) quartz differ to a significant extent from
19 cryptocrystalline rocks in their mechanical properties that affect fracture formation (Callahan et al.
20 1992; Domanski et al. 1994; Mourre 1996; de Lombera Hermida 2009; Driscoll 2010; Tallavaara et al.
21 2010; de Lombera-Hermida and Rodríguez-Rellán 2016; Rodríguez-Rellán 2016). This has been
22 established in technological studies aimed at understanding the seemingly chaotic fragmentation of
23 quartz flakes during knapping and the differences between the technological attributes of quartz
24 and flint or chert flakes (Callahan et al. 1992; Driscoll 2010, 2011a; Tallavaara et al. 2010; Manninen
25 2016; Tardy et al. 2016).

26 We believe that there is a need for a solid experimental foundation that acknowledges these
27 idiosyncrasies (see Knutsson 1988; Callahan et al. 1992; Domanski et al. 1994; Mourre 1996; de
28 Lombera Hermida 2009; Tallavaara et al. 2010; Rodríguez-Rellán 2016). We present the results of a
29 functional analysis of 91 experimental armatures made on automorphic quartz and xenomorphic
30 quartz. Our aim is to gain a preliminary understanding of the specifics of impact wear formation on
31 these raw materials using their key physical and mechanical properties discussed in recent
32 archaeological literature as a frame of reference. In addition to evaluating the implications of these
33 properties on projectile identification on the basis of our experimental data, we compare damage
34 patterns on three different projectile types – barbs, transverse points, and convergent points – and
35 discuss the possibilities of identifying these different armature types archaeologically based on use-
36 wear evidence.

37 Our sample partly derives from the experiments designed to understand impact damage
38 formation on small quartz artefacts from the Howiesons Poort layers of Sibudu Cave (de la Peña et
39 al. 2018), and was complemented with further experiments. The goal of these exploratory
40 experiments was to produce material that can serve as a realistic (even if preliminary) referential
41 basis for the analysis of archaeological quartz armatures. To reach this goal, we used materials that
42 would have been available in prehistory, and included several armature types to be able to cover the
43 variability we assume existed in the past. In addition, we analysed a number of transverse and
44 oblique arrowheads from an earlier experiment (Seppä 1995) that had a slightly different setup. We
45 examine the characteristics and frequency of impact damage, MLITs, and other microwear on these
46 armatures paying special attention to the consequences of hafted use. We show that the particular
47 properties of quartz affect fracture patterns also on microscale, and point out possible difficulties
48 and sources of confusion in quartz projectile identification.

1
2
3
4
5
6
7
8
9
10
11
12
13
14
15
16
17
18
19
20
21
22
23
24
25
26
27
28
29
30
31
32
33
34
35
36
37
38
39
40
41
42
43
44
45
46
47

2 Background

Projectile identification very often relies on the detection of so-called diagnostic impact fractures (DIFs). This approach builds on experimental studies that have dealt with projectiles in flint and flint-like rocks (e.g. Odell 1978; Barton and Bergman 1982; Moss and Newcomer 1982; Odell and Cowan 1986; Geneste and Plisson 1990). It is based on the observation that certain types of breaks recur in projectile use and rarely result from other processes (knapping, other types of tool use, taphonomic events), and can therefore be considered diagnostic of impact (Fischer et al. 1984). The reliability of the method as well as the consistency of the criteria and terminology used by different analysts have recently been called into question (Rots and Plisson 2014; Coppe and Rots 2017), but it still serves as a basis in many projectile studies.

Pargeter has discussed DIFs on quartz in several recent publications (Pargeter 2011, 2013; Pargeter et al. 2016). He experimented with various rock types common at South African sites, including xenomorphic (vein) quartz (Pargeter 2013). The results led him to conclude that DIFs occur on all rock types examined, and that tool use is thus a factor that overrides lithic raw material variability in macrofracture formation (Pargeter 2013). In a more recent study (Pargeter et al. 2016), Pargeter and colleagues tested the possibilities of distinguishing between experimental quartz arrow and spear heads using the macrofracture method. They report high frequencies of DIFs on their experimental transversely hafted arrow and spear heads (Pargeter et al. 2016: fig. 8 and table 3). While they acknowledge that some of the differences between their dataset and those published earlier can be attributed to the variability in raw materials used in the experiments, they do not explicitly discuss the impact of the properties of quartz on fracture formation.

We agree that approaches where large samples are coupled with appropriate quantification procedures and statistical treatment of the data, such as the one proposed by Pargeter et al. (2016), should be encouraged in projectile studies. However, all methods that aim at reconstructing weapons involving quartz components should in our view rely on a firm understanding of the particular fracture mechanical properties of quartz and their effect on the appearance of impact damage. Only after the particularities of break and damage formation are understood can these features be quantified in a way that yields archaeologically relevant information. In the case of quartz, one of the questions that remain is whether or not the structural properties of the raw material intervene with fracture formation to such an extent that some of the variation in feature characteristics (dimensions) can be considered random and therefore not useful for understanding weapon systems.

Interestingly, Fernández-Marchena et al. (2017) report an absence of DIFs in their pilot study that examined projectile tips made of automorphic (crystal) quartz. Since they do not report their sample size and since the definitions of DIFs often vary from one analyst to another (for a critical review of literature, see Coppe and Rots 2017), the significance of this absence is difficult to evaluate. Even so, both Pargeter et al.'s and Fernandez-Marchena et al.'s studies seem to suggest that the differences between quartz and cryptocrystalline rocks are not trivial for impact damage formation.

3 Terminology

For distinguishing between the two main types of macrocrystalline quartz, we apply here the terms 'automorphic' and 'xenomorphic' following Mourre (1996) and Rodríguez-Rellán (2016). Automorphic quartz occurs as hexagonal crystals of varying sizes, and is usually referred to as rock crystal, crystal quartz, or hyaline quartz in archaeological literature (Rodríguez-Rellán 2016). Xenomorphic quartz, commonly called vein quartz or milky quartz, is a polycrystalline aggregate

1 where the individual crystals lack the distinctive shape typical of automorphic quartz (Rodríguez-
2 Rellán 2016), which usually gives the quartz a less glassy and grainier appearance. We consider the
3 terms automorphic and xenomorphic the least confusing of the ones in current use since
4 automorphic crystals can occur in quartz veins (de Lombera Hermida 2009), making 'vein quartz' a
5 rather non-descriptive (albeit established) term.

6 For describing macroscopic damage from impact, we use the term 'break' to refer to a
7 fracture that cuts the piece from one edge to another, while removals limited to one edge are
8 considered 'scars'. A recent review of literature has shown that the term 'burination' is used for a
9 variety of features and that the results of individual studies are not therefore easily comparable
10 (Coppe and Rots 2017). Here, the term is used purely for its descriptive value to separate "burin-
11 like" features from the rest, and the type of feature (primary or secondary removal) referred to is
12 each time specified in the text.

13 14 4 Macroscopic and microscopic wear on quartz

15 *4.1 Mechanical properties and macrotrace formation*

16 Wear formation on quartz is not easily comparable to flint (see Knutsson 1988; Knutsson et al.
17 2015b; Ollé et al. 2016). Both automorphic and xenomorphic quartz have particular mechanical
18 properties that cause them to behave differently from cryptocrystalline rocks under mechanical
19 stress. These qualities have been acknowledged and discussed in the recent decades in the context
20 of technological analysis (for a summary, see de Lombera-Hermida and Rodríguez-Rellán 2016), but
21 the role of each physical property in the outcome of the knapping (or other fracturing) process is still
22 not understood in detail. Continuity (measure of amount of cracks and flaws), isotropy (measure of
23 directional properties) (Domanski et al. 1994; Rodríguez-Rellán 2016) and homogeneity all play a
24 role in the predictability of fractures in quartz (Rodríguez-Rellán 2016). In terms of these properties,
25 the relationship between automorphic and xenomorphic quartz is not strictly hierarchical.
26 Xenomorphic quartz can for example be more isotropic than automorphic quartz (Rodríguez-Rellán
27 2016).

28 29 4.1.1 Automorphic quartz

30 While fracture formation on automorphic quartz can be more predictable and features formed
31 through conchoidal fracture are more pronounced than on xenomorphic quartz, crystal quartz does
32 not behave in the same way as flint (Driscoll 2010). Further, only the apical parts of crystals can be
33 considered isotropic and homogenous. The rest of the crystal is anisotropic due to presence of
34 cleavage planes and diaclasis (Mourre 1996; de Lombera Hermida 2009; Fernández-Marchena and
35 Ollé 2016; Rodríguez-Rellán 2016; Tardy et al. 2016), and especially the basal parts of the crystals
36 often have flaws and impurities that significantly affect the fracturing qualities of the raw material
37 (de Lombera Hermida 2009; Rodríguez-Rellán 2016).

38 The direction in which the quartz is knapped (parallel, oblique, or perpendicular to the
39 length of the crystal) affects the extent to which the features responsible for anisotropy interfere
40 with fracture propagation (Mourre 1996; Tardy et al. 2016), and the strength of bonds between
41 molecules is not the same in all directions (Rodríguez-Rellán 2016). Anisotropy is manifested in
42 features such as ripple amplification, which appears when the crystal is knapped in the direction of
43 its length or its thickness and disappears when the direction is oblique to the length (Tardy et al.
44 2016: fig. 17). These qualities can be hypothesized to also affect impact damage, for instance the
45 morphometrics of removals.

1 Another recent study reports that lancets (hackles), often pronounced in automorphic
2 quartz, affect the shape of microscopic use-related scars (Fernández-Marchena and Ollé 2016), but
3 the impact of hackles on the formation of impact scars remains to be evaluated.
4

5 4.1.2 Xenomorphic quartz

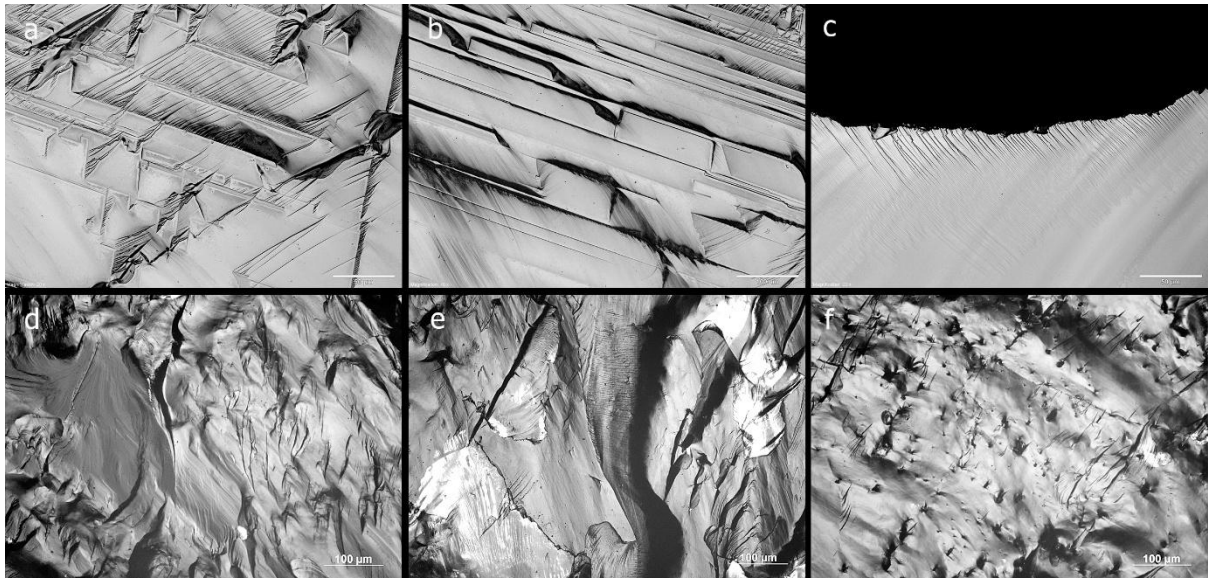
6 Fracture patterns in xenomorphic quartz can be quite complex. The material shows both conchoidal
7 and uneven fracture (de Lombera Hermida 2009). Its tensile and compressive strength is relatively
8 low, and qualities such as the presence of internal planes and flaws, the anisotropy of crystals, and
9 the grainy structure can result in irregular and unpredictable fracture patterns (Callahan et al. 1992;
10 Domanski et al. 1994; de Lombera Hermida 2009; Tallavaara et al. 2010; de Lombera-Hermida and
11 Rodríguez-Rellán 2016).

12 In good-quality flint a fracture propagates through the material and ideally results in the
13 detachment of a single intact flake with a clear cone initiation, whereas in quartz the energy is
14 dispersed throughout the material as the crack propagates along existing planes of weakness in
15 multiple directions (de Lombera Hermida 2009). The effect is twofold: quartz flakes often fragment
16 upon detachment, and typical features such as bulbs of percussion tend to be absent or diffuse on
17 them (Callahan et al. 1992; Rankama 2002; Tallavaara et al. 2010). The unwanted fracture
18 propagation along discontinuities in the material can occur not only during blank production but also
19 shaping (Mourre 1996), which suggests that this behaviour also has an effect on impact break and
20 damage formation.

21 We predict that in impact fracture formation the above-mentioned properties of
22 xenomorphic quartz will result in breakage along fault planes and other zones of weakness, in
23 removals with irregular and/or diffuse and consequently hard-to-read morphologies, and in frequent
24 and unpredictable interruption of fracture propagation. Even though these properties do not
25 necessarily result in the absence of “diagnostic” breaks and removals in quartz (cf. Pargeter 2013;
26 Pargeter et al. 2016), they can be expected to increase the variability in feature attributes and
27 dimensions, and also to yield lower frequencies of “diagnostic” breaks and removals when compared
28 to rock types with a more predictable behaviour.
29

30 4.2 Microwear

31 Under high magnification, one of the most striking features of quartz is the highly varied structure of
32 its surfaces (Fig. 1a-f; see also Fernández-Marchena and Ollé 2016 for similar features on
33 automorphic quartz). This abundance of natural features can be problematic especially for analysts
34 accustomed to the more homogenous microtopography of cryptocrystalline rocks such as flint. The
35 existence of natural linear surface features has been repeatedly pointed out by analysts since the
36 origins of high magnification analysis of quartz (e.g. Fullagar 1986; Knutsson 1988). Nevertheless,
37 these features, visible as sets of fine parallel lines under the microscope (Fig. 1c), have become
38 misinterpreted as use-wear also in recent studies. This is the case in Lombard’s study on Howiesons
39 Poort segments from Sibudu. These artefacts were argued to be transverse arrowheads partly on the
40 basis of linear features with suitable orientations found at the tools’ edges (Lombard 2011). These
41 features are, in fact, commonly occurring natural formations, as already pointed out in other studies
42 dealing with quartz (Fernández-Marchena and Ollé 2016; de la Peña et al. 2018).
43



1
2
3 **Fig. 1** Examples of the varied microtopography of automorphic (crystal) and xenomorphic (vein) quartz
4 (unused pieces). a. Automorphic quartz, original magnification 200×, scale bar 50µm. b. Automorphic quartz,
5 original magnification 100×, scale bar 100µm. c. Natural linear surface features oriented obliquely to the edge
6 on an experimental unmodified and unused automorphic quartz flake (de la Pena et al. 2018, fig. 23). d.-f.
7 Xenomorphic quartz, original magnification 200×, scale bars 100µm (for a description of the microscopic
8 structure of xenomorphic quartz, see Knutsson 1988)
9

10 The formation of actual microwear on quartz is characterised by quick appearance of chipping,
11 rounding (microchipping) and cracking of the outermost edges accompanied with the formation of
12 linear features, and relatively slow and limited development of polish that only forms when working
13 certain materials (Knutsson 1988). This is due to the poor response of quartz to high pressure, which
14 gives rise to edge fracturing and subsurface damage at the expense of abrasive processes, making
15 microwear on quartz very different from wear on flint (de Lomberra Hermida 2009). Linear features
16 form the bulk of use-wear on quartz and are easily detectable under appropriate magnifications. It
17 has been proposed that they form either through brittle fracture wear, in which case they are linear
18 arrays of surface and subsurface cracks, or through plastic deformation (Kamminga 1982; Knutsson
19 1988; Derndarsky and Ocklind 2001).

20 K. Knutsson's experimental work employing scanning electron microscope analysis and
21 surface etching led him to conclude that the wear formation process on quartz is as a whole a
22 combination of micro-fracturing, material fatigue, silica precipitation, dissolution, plastic
23 deformation, polishing and phase transformation (Knutsson 1988; Knutsson et al. 2015b). When the
24 co-occurrence of different types of wear features (striations, plastic deformations, polish, etc.;
25 Knutsson 1988) is treated statistically, it seems that certain worked materials form clusters
26 according to their physical and chemical properties, and that given associations of wear features can
27 thus serve as indications of various worked materials (Knutsson et al. 2015b). In the context of
28 projectiles, different forms of micro-fracturing together with linear features can be said to be the
29 main interest, as these forms of wear are quick enough to develop even through short contact with
30 the worked material.
31

32 5 Material and methods

33 5.1 Material

1 We analysed a total of 91 experimental armatures under low magnification and 76 of them under
 2 high magnification. This material comes from two sets of experiments: the ones conducted at
 3 TraceoLab (a total of 87 armatures shot, 11 of which could not recovered after the experiment,
 4 leaving 76 for analysis) and an earlier experiment (Seppä 1995) from which 15 armatures were
 5 analysed (Table 1).

6 The main body of experimental material in this study consists of barbs and transverse
 7 points. This choice was motivated by the fact that these armature types have received most
 8 attention in recent literature dealing with archaeological contexts where quartz was used
 9 abundantly (Lombard 2011; Knutsson et al. 2015a; Pargeter et al. 2016; de la Peña et al. 2018). A
 10 majority of the experimental armatures presented here derive from the experiments done in the
 11 context of the study of micro-notches from Sibudu (de la Peña et al. 2018). For the purposes of the
 12 present methodological study, the transverse point sample was expanded to include morphologies
 13 more similar to Mesolithic quartz arrowheads to further evaluate impact damage patterns on
 14 transverse points. These armatures are transverse points in the strict sense: the alignment of the
 15 cutting edge is perpendicular to the axis of the arrow. The armatures from Seppä's (1995)
 16 experiment are oblique and transverse points. They were examined to gain a preliminary
 17 understanding of the possible effects of cutting edge alignment on damage formation. Finally, ten
 18 convergent tips of morphologies roughly similar to those of the barbs and segments were added to
 19 the sample to understand possible sources of confusion in identifying armature orientation on the
 20 basis of macroscopic and microscopic wear (Fig. 2).

21
22

Projectile type	Production		Analysis		Σ analysed	Σ lost	Σ shot
	Knapper	Method	Low magn.	High magn.			
Barbs / automorphic	CL	freehand	14	14	14	4	18
Barbs / xenomorphic	CL	freehand	26	26	26	1	27
Transverse / automorphic	CL	freehand	11	11	11	3	14
Transverse / xenomorphic	CL	freehand	16	16	16	2	18
Transverse / automorphic	JS	bipolar	8	0	8	0	8
Transverse / xenomorphic	JS	bipolar	7	0	7	0	7
Convergent / automorphic	CL	freehand	4	4	4	1	5
Convergent / xenomorph	CL	freehand	5	5	5	0	5
Total			91	76	91	11	102

23
24
25

Table 1 Summary of the experimental material included in the study

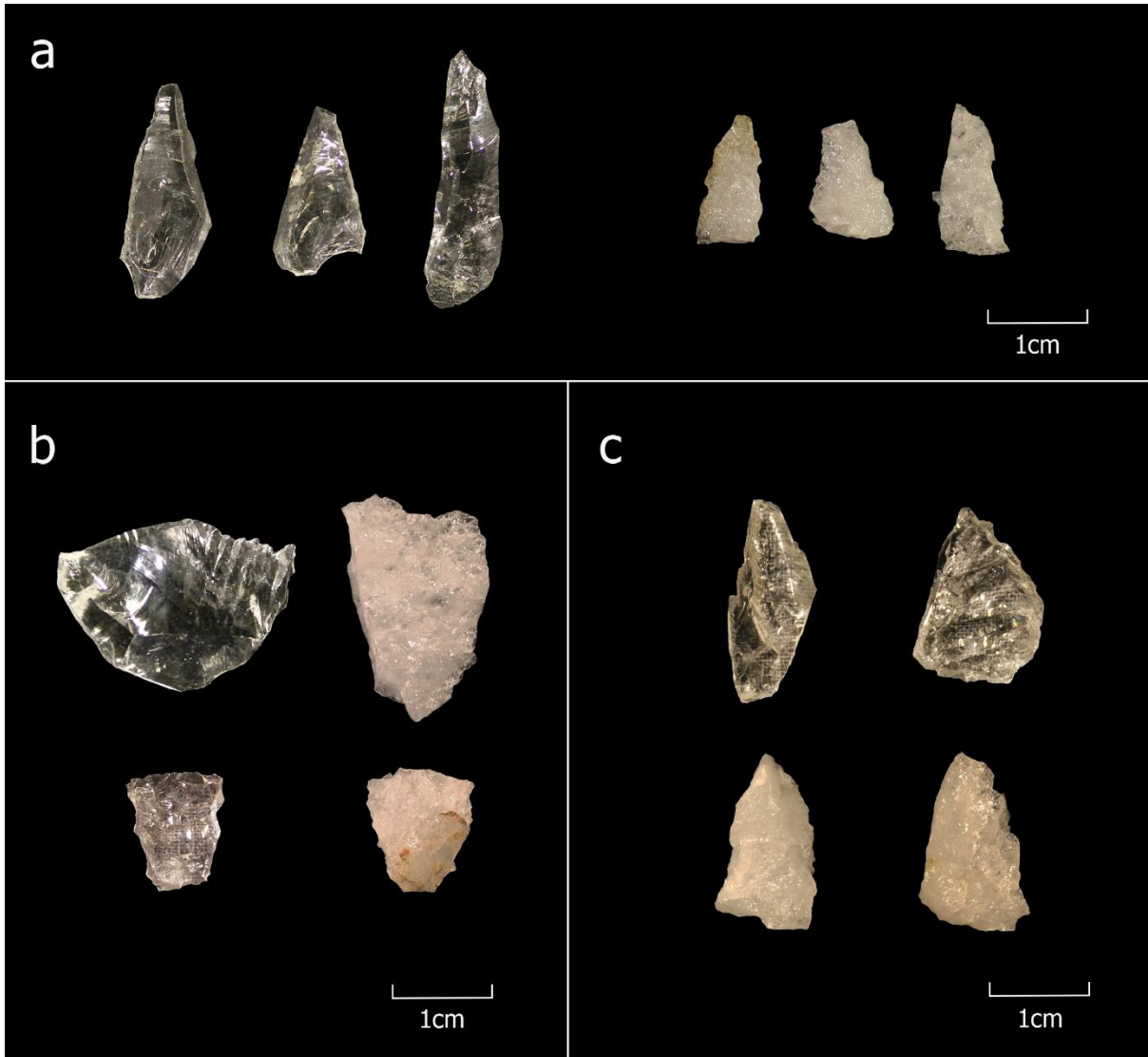


Fig. 2 Examples of experimental armatures before hafting (all dorsal views). a: barbs (Exp. 86/48 and 53), b: transverse points (86/65, 84, 88 and 91), c: convergent points (86/95, 97, 100 and 103)

Unmodified and unused flakes and fragments from earlier knapping experiments were used as a control sample for addressing specific issues such as damage formation during bipolar knapping, and secondary scarring associated with breaks. This material includes both automorphic and xenomorphic quartz, and represents two main blank production methods, bipolar and freehand platform flaking.

5.2 Experimental setup

The blanks for the armatures were produced by experienced knapper Christian Lepers (CL) from unidirectional platform cores using freehand percussion, and some of them were further shaped by minimal retouching of the non-active parts to make the tools easier to haft. Eighteen barbs were made out of automorphic quartz and 27 out of xenomorphic quartz, whereas for the transverse points, the ratio was 14 to 18, respectively. Five tips with convergent distal edges were made per raw material category, resulting in a total of ten tips.

The armatures were photographed before hafting and examined under low magnification. All production-related features (retouch, breaks, scarring, crushing, etc.) were noted on photos to

1 ensure that they would not be confused with impact wear. Also zones with macroscopically visible
2 cracks and other flaws – expected to be fragile and thus susceptible to irregular breakage upon
3 impact – were marked on the photos when observed.

4 The barbs were attached laterally on self-pointed wooden arrows, always in aligned sets of
5 three. Two of the 15 shafts used had grooves made for the barbs. For five arrows, including the two
6 grooved ones, only sinew was used for attaching the barbs. Five arrows were put together using
7 adhesive only. For the remaining five arrows, both sinew and adhesive were used (Fig. 3a-c).
8 Throughout the experiment, the adhesive used was a mixture of natural spruce resin (70%) and
9 beeswax (30%).

10



11

12

13 **Fig. 3** Examples of barbed arrows before the experiment. Left: sinew and adhesive (Exp. 86/45), middle:
14 adhesive (spruce resin and beeswax) only (86/51), right: sinew only (86/53)

15

16 The transverse points and the convergent points were fitted at the extremities of split wooden
17 shafts. For six points, only sinew was used. Two points were hafted using adhesive only. The
18 remaining 24 were mounted using a combination of sinew and adhesive.

19 The arrows were photographed before the experiment and then shot by CL from a distance
20 of 10 meters with a 47-pound flat bow made of elm wood (29-inch draw distance). A pony skeleton
21 encased in ballistic gel moulded in the form of the animal and covered with a stretched, fresh hide

1 was used as a target (for details see Coppe and Rots 2017). Each arrow was shot three times at most.
2 If the armatures broke or detached sooner, the experiment was stopped.

3 Documentation sheets were used to record for example the penetration depth of the
4 projectile, possible breakage and/or detachment of the lithic armature, and the arrow's position in
5 the target. All arrows were photographed also after the shoot to allow a better understanding of
6 use-wear formation.

7 The transverse and oblique arrowheads coming from Seppä's experiment are made of
8 xenomorphic (milky) quartz and of automorphic (rose) quartz. The armatures were hafted with
9 sinew bindings and shot with a 39-pound flat bow and a 51-pound long bow. This experiment was
10 designed to evaluate the performance of the arrowheads, and included a preliminary test using a
11 paraffin target and a more actualistic experiment where a roe deer carcass was used. The shooting
12 distances were 15 and 10 metres, respectively (Seppä 1995).

13 14 *5.3 Analysis*

15 Our analytical approach combines low and high magnifications in a phased procedure. Low
16 magnifications have been previously used in quartz studies (e.g. Broadbent and Knutsson 1975;
17 Rankama 2002), but practically all extensive methodological work has been done in the field of high
18 magnification analysis (e.g. Knutsson 1988), and the combination of the two approaches has been
19 advocated only recently (Taipale 2012; Taipale et al. 2014; Rots et al. 2017; de la Peña et al. 2018).

20 Low magnification analysis was done using Olympus and Zeiss stereomicroscopes (Olympus
21 SZX7, magnifications 8–56×, and Zeiss Stemi, magnifications 6.5–50×). The observed features were
22 compared with notes on production-related features, and the presence, location, and basic
23 characteristics of impact-related breaks and damage were then recorded. For barbs, where break
24 and scar patterns are quite complex especially due to scars caused by bindings and the contact of
25 detached barbs with each other on impact (see below), a more detailed recording was employed
26 using an attribute-based documentation system recently developed for projectile analysis (see
27 Coppe and Rots 2017). The main break types referred to in sections 6.4–6 are shown in Fig. 4. The
28 macroscopic features were photographed with a Zeiss Macro-Zoom microscope V16 (magnifications
29 5.6–180×) and stacked in Helicon Focus.

30

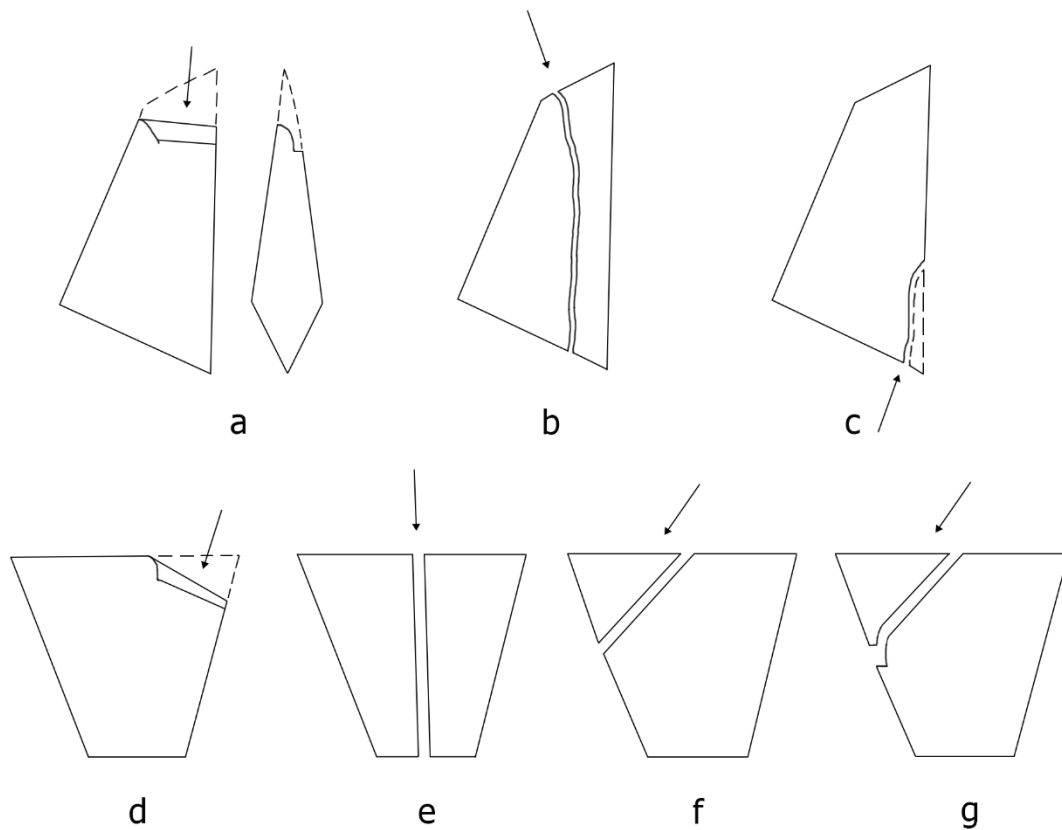


Fig. 4 Different types of breaks observed on experimental armatures (see sections 6.4–6 and tables within). a. Transverse bending-initiated step-terminating surface-to-surface break on a barb/tip. b. A longitudinal edge-to-edge break on a barb. c. A longitudinal removal (“burination”) on a barb. d. An oblique (nearly transverse) surface-to-surface break on a transverse point. e. A longitudinal edge-to-edge break on a transverse point. f. An oblique edge-to-edge break on a transverse point. g. A step-terminating oblique edge-to-edge break on a transverse point. For description of other impact-related traces such as spin-offs, see e.g. Coppe and Rots 2017

Spotting small lateral removals on xenomorphic quartz is not always easy, whereas on automorphic quartz, even the smallest scars can be observed and recorded in detail without difficulty. One outcome of the structural properties of xenomorphic varieties is the generally varied surface topography of knapped quartz. When coupled with the high reflectivity of the raw material, this quality makes the identification and characterisation of retouch and other removals on xenomorphic quartz edges sometimes difficult. These problematics are well illustrated by blind tests where participants on the one hand identified unmodified xenomorphic quartz pieces as retouched implements and on the other hand sometimes severely struggled with detecting retouch (Lindgren 1998; Driscoll 2011b). These results suggest that caution will also be needed when identifying used edges solely on the basis of macroscopic features, as some irregularities formed during blank detachment can mimic secondary removals.

The projectiles were examined under high magnification using an Olympus metallurgical microscope BX51M (magnifications 100–1000×) and a Zeiss Axiomager (magnifications 50–500×) equipped with polarising filters and DIC to record microscopic linear impact traces (MLITs) (Moss 1983) and other impact-related features. Prior to high magnification analysis, the pieces were cleaned of resin and other residues. They were first dipped in freshly boiled water to soften the

1 resin, most of which was then wiped off with cotton. If needed, they were next immersed in weak
2 NaOH solution (1 mol/l) for two minutes and the partly dissolved remains of resin were removed in
3 an ultrasonic bath using tap water, or alternatively wiped off with cotton dipped in acetone. The
4 treatments were repeated when necessary. During analysis, ethanol and acetone were frequently
5 used to remove handling grease.

6 Surfaces of xenomorphic quartz are often irregular, which leads into "blind spots" during
7 analysis. Magnification of 500× was therefore abundantly used to ensure that all the relevant areas
8 could be properly observed despite the varied microtopography. For both raw material categories,
9 the presence of original crystal surfaces and recrystallization surfaces, sometimes formed on quartz
10 as the result of instability in quartz veins due to tectonic activity (Driscoll 2010; Fernández-Marchena
11 and Ollé 2016), occasionally posed limitations for observations. These surfaces were excluded from
12 high magnification analysis and their location recorded together with other data.

13 The main set of data discussed in the following sections comes exclusively from the
14 experiments done at TraceoLab. This allows us to keep certain critical variables (bow, target,
15 shooting distance) constant. Seppä's (1995) arrowheads serve here as a point of comparison that
16 permits evaluating the representativeness of the main results. These armatures are briefly discussed
17 in section 6.5 and are not included in the tables. The material from Seppä's experiment was not
18 examined under high magnification since the purpose was to evaluate whether the general damage
19 patterns on oblique arrowheads differ from those on transverse ones. This experiment was not
20 designed for microwear analysis, and the armatures were not examined microscopically before the
21 experiment. Therefore, only features that are obviously impact-related – i.e. breaks and larger
22 damage – are considered here.

23 A number of pieces with macroscopic damage that was particularly difficult to characterise,
24 interpret, or photograph were selected for more detailed analysis and imaging using a JEOL IT300
25 SEM in low vacuum mode. Several researchers have used scanning electron microscopy in exploring
26 and documenting wear on quartz and similar materials, and it has obvious advantages (e.g. Knutsson
27 1988; Márquez et al. 2016; Ollé et al. 2016). We limit its use here to the documentation and further
28 analysis of certain ambiguous features observed under low magnification.

29 Our approach here is essentially qualitative. We describe a number of relevant microscopic
30 features in detail to illustrate the particularities in the behaviour of quartz. While we in the following
31 sections summarise the frequencies of certain impact features in our experimental samples, this is
32 only done to provide the reader with an overview of the wear patterns and to allow a discussion on
33 how different features co-occur. The (sub)samples presented here are too small for reliable
34 statistical analysis. The exclusion of statistics at this stage, however, is primarily motivated by a
35 conscious methodological choice. Treating the data statistically would mean operating on the level
36 of feature frequencies, which translates into DIFs. We do not believe that focusing on individual
37 features is an advisable approach, and in fact argue that this is an important methodological issue
38 that requires further attention in the field of projectile studies (see Rots and Plisson 2014; Coppe
39 and Rots 2017).

40 41 6 Results

42 *6.1 Projectile performance*

43 The outcomes of the projectile experiments done at TraceoLab are summarised in Tables 2–4. For
44 the 13 barbed arrows that successfully entered the target, penetrations from 1cm up to 19cm were
45 measured. Seventeen of the arrows tipped with transverse points successfully pierced the skin and
46 entered the target, causing wounds between 7cm and 19.5cm in depth. For the eight arrows with
47 convergent tips, the depth of penetration varied between 6.5 and 16.5cm.

1

Exp. 86/ID	Quartz type	Hafting	Nr of shots	Contact material				Outcome
				skin	gel	bone	wall	
44a-c	Automorphic	Adhesive	1					Explosion, barbs lost
45a-c	Automorphic	Sinew + adhesive	2	•	•			Two barbs de-hafted
46a-c	Automorphic	Sinew	2	•	•			Two fragments remain in shaft
47a-c	Automorphic	Sinew	1	•	•			Barbs collided
48a-c	Automorphic	Sinew + adhesive	2	•	•			One fragment remains in shaft
49a-c	Automorphic	Adhesive	1	•	•			One barb de-hafted
50a-c	Xenomorphic	Sinew	1	•	•			Two barbs de-hafted
51a-c	Xenomorphic	Sinew + adhesive	1	•	•			One barb de-hafted
52a-c	Xenomorphic	Sinew + adhesive	1	•	•			One barb fragmented
53a-c	Xenomorphic	Sinew, in groove	1	•				All barbs de-hafted
54a-c	Xenomorphic	Sinew + adhesive	3	•	•	•		All barbs still attached
55a-c	Xenomorphic	Adhesive	1	•	•	•		Barbs still attached, one broken
56a-c	Xenomorphic	Adhesive	1	•	•			Barbs still attached, one broken
57a-c	Xenomorphic	Sinew, in groove	3	•	•			Two fragments remain in shaft
58a-c	Xenomorphic	Adhesive	1	•	•	•		One barb de-hafted

2

3

Table 2 Outcome of the barb experiment (three barbs per arrow, a-c)

4

Exp. 86/ID	Quartz type	Hafting	Nr of shots	Contact material				Outcome
				skin	gel	bone	wall	
62	Automorphic	Sinew + adhesive	1	•			•	Point broken in shaft
63	Automorphic	Sinew + adhesive	1				•	Point broken in shaft
64	Automorphic	Sinew	1				•	Point lost
65	Automorphic	Sinew	1	•	•	•		Point damaged and de-hafted
66	Automorphic	Sinew + adhesive	1	•				Point broken in shaft
67	Automorphic	Sinew	2	•	•		•	Point broken in shaft
68	Xenomorphic	Sinew + adhesive	1				•	Point broken and de-hafted
69	Xenomorphic	Sinew	3	•	•	•		Point lost
70	Xenomorphic	Sinew + adhesive	1	•				Point broken and de-hafted
71	Xenomorphic	Sinew	1	•	•			Point damaged in shaft
72	Xenomorphic	Sinew	1	•				Point damaged in shaft
73	Xenomorphic	Sinew + adhesive	1	•	•	•		Point broken in shaft
74	Xenomorphic	Sinew + adhesive	1	•				Point damaged and de-hafted
75	Xenomorphic	Sinew + adhesive	1	•				Point broken in shaft
76	Xenomorphic	Sinew + adhesive	1	•	•	•		Point broken in shaft
77	Xenomorphic	Adhesive	1	•	•	•		Point broken and de-hafted
78	Xenomorphic	Adhesive	1	•	•			Point broken and de-hafted
79	Xenomorphic	Sinew + adhesive	1	•	•	•		Point broken in shaft
80	Automorphic	Sinew + adhesive	1	•	•	•		Point lost
81	Automorphic	Sinew + adhesive	1	•	•	•		Point damaged and de-hafted?
82	Automorphic	Sinew + adhesive	1	•	•			Point broken in shaft
83	Automorphic	Sinew + adhesive	1					Point de-hafted before impact
84	Automorphic	Sinew + adhesive	1	•	•			Point de-hafted
85	Automorphic	Sinew + adhesive	1	•				Point broken and de-hafted

86	Automorphic	Sinew + adhesive	1	●	●	●		Point broken in shaft
87	Automorphic	Sinew + adhesive	1	●				Point broken in shaft
88	Xenomorphhic	Sinew + adhesive	1	●				Point broken in shaft
89	Xenomorphhic	Sinew + adhesive	2	●	●	●		Point broken and de-hafted
90	Xenomorphhic	Sinew + adhesive	1	●	●	●		Point de-hafted, shaft broken
91	Xenomorphhic	Sinew + adhesive	1	●				Point broken and de-hafted
92	Xenomorphhic	Sinew + adhesive	1	●				Point damaged, moved in shaft
93	Xenomorphhic	Sinew + adhesive	2	●	●			Point broken in shaft

1
2
3

Table 3 Outcome of the transverse point experiment

Exp. 86/ID	Quartz type	Hafting	Nr of shots	Contact material				Outcome
				skin	gel	bone	wall	
94	Automorphic	Adhesive	1	●	●	●		Point damaged in shaft
95	Automorphic	Sinew + adhesive	1	●	●	●		Point broken in shaft
96	Automorphic	Adhesive	1	●	●	●		Point broken in shaft
97	Automorphic	Sinew + adhesive	1	●	●	●		Point damaged in shaft
98	Automorphic	Adhesive	1	●	●	●		Point lost
99	Xenomorphhic	Adhesive	1	●				Point de-hafted
100	Xenomorphhic	Sinew + adhesive	2	●	●	●		Point broken in shaft
101	Xenomorphhic	Sinew + adhesive	3	●	●	●		Point broken in shaft
102	Xenomorphhic	Adhesive	1	●		●		Point broken in shaft
103	Xenomorphhic	Sinew + adhesive	1	●	●	●		Point broken in shaft

4
5
6

Table 4 Outcome of the tip experiment

7 It appears that for the transverse arrows, the morphology of the lithic armature affected success
8 rate more than it did for the barbs. In the case of arrows mounted with barbs, the wooden point
9 pierced the skin first, whereas for arrows tipped with transverse points, the properties of the cutting
10 edge and other morphological aspects were crucial for success. Some points that failed to pierce the
11 skin displayed clear morphological disadvantages, such as relatively thick portions right behind the
12 cutting edge due to the proximity of the butt and the bulb of the blank. In some cases, however,
13 these disadvantages could be overcome, and the arrow was shot deep into the target despite the
14 less-than-ideal distal morphology. This probably has to do with the angle of impact and the variation
15 in the thickness of the skin stretched over the target.

16 While acknowledging that the morphometric variability within the projectile categories is
17 quite substantial (Fig. 2), and that the division of the transverse points into segments and Mesolithic
18 points is somewhat artificial due to limited amount of retouch and high variability in blank shapes, it
19 is interesting to note that the small sample examined here may suggest differences among success
20 rates of these general morphologies. The success rate is highest for the barbs, suggesting that this
21 hafting mode allows for the largest variability in blank morphometrics without significant influence
22 on the outcome. It has to be stressed, however, that the basic functioning of these arrows
23 significantly differs from the other three categories: the sharpened wooden tip is the part that first
24 pierces the skin, making these arrows somewhat more standardised in design in comparison to the
25 rest of the sample. While the sample remains small, it seems obvious that the arrows on which the
26 barbs were fixed with only sinew performed worse than those where adhesive was used. The sinew-
27 bound barbs detached from their shafts in several cases upon impact and thus did not contribute to
28 the size of the wound.

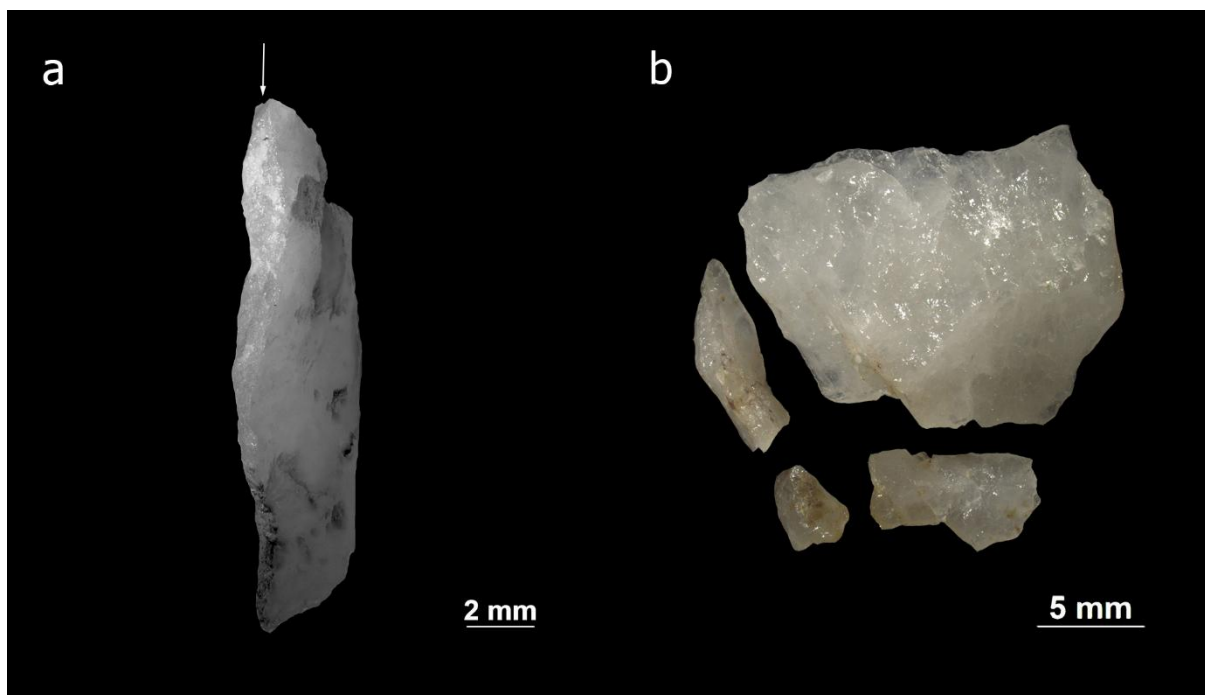
1 When the special case of barbed arrows is left aside, the rest of the sample shows the
2 highest success rate for tips (8/9), second highest for segment-shaped transverse points (9/12), and
3 the lowest for the remaining transverse arrows (8/16). The samples are small, but these
4 observations seem to suggest that as far as unmodified or minimally retouched blanks go, selecting
5 flakes with convergent distal morphologies is a safer choice than selecting ones with a transverse
6 cutting edge. While these results are preliminary and can partly be attributed to other variables than
7 point morphology, they may have interesting implications for blank selection and projectile design. It
8 seems that in the case of transverse arrowheads, the morphology of the blank has to be more
9 carefully selected for and/or adjusted than in the case of tips with convergent distal extremities. This
10 may in part explain the observation that Mesolithic transverse and oblique points are a relatively
11 standardised artefact category in quartz assemblages where the proportion of formal tools is
12 otherwise low (see Manninen and Knutsson 2011; Manninen and Tallavaara 2011).

13

14 *6.2 Trace formation and identification: general observations*

15 As expected, xenomorphic quartz in particular is somewhat unique in terms of trace formation and
16 analysis. Impurities that may affect fracture patterns can be sizeable and frequent. This is illustrated
17 by a barb where a longitudinal break (“burination”) propagated along an impurity in the material
18 (Fig. 5a), and by a transverse point where the proximal end shattered along impurities, cracks, and
19 recrystallization planes (Fig. 5b).

20



21

22

23 **Fig. 5 a.** A longitudinal break (“burination”) that followed an impurity in the raw material (barb 86/55a,

24 xenomorphic quartz). Original magnification 10×. b. An experimental transverse arrowhead (86/70,

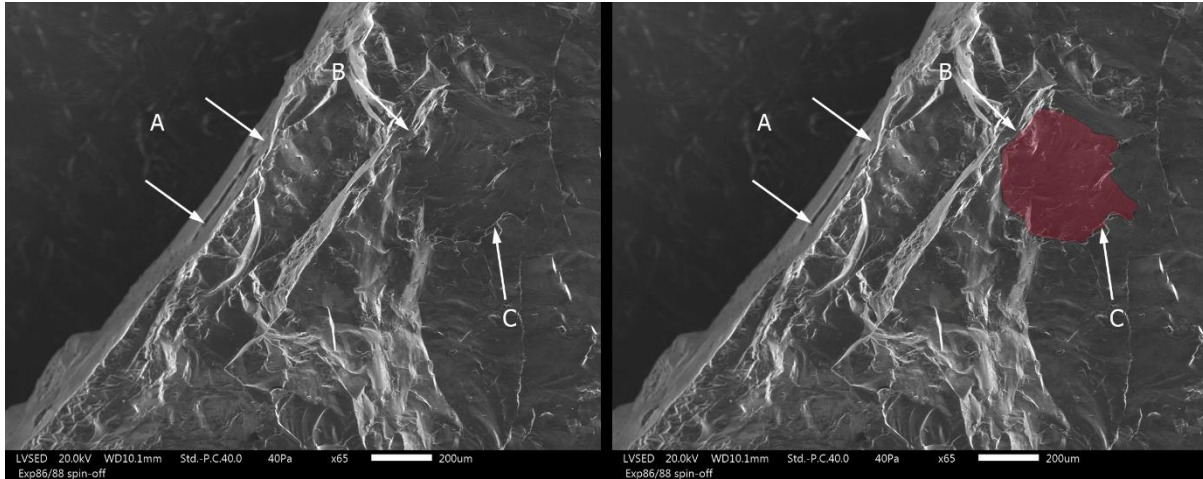
25 xenomorphic quartz) showing breakage along flaws and irregularities in the material

26

27 SEM analysis offers further evidence of the idiosyncratic behaviour of quartz under mechanical
28 stress. For instance, on one of the pieces (86/88), possible deep step-terminating spin-offs were
29 recorded, but their initiations were judged either very diffuse or absent, and it was unclear whether
30 they were truly secondary damage associated with the break and not simply surface irregularities
31 formed during knapping and cut by the subsequent impact break. The SEM image of the area

1 suggests that the observed features do initiate from the break surface, but the area seems to show a
2 combination of flaw-controlled fracture propagation and fully developed conchoidal fracturing on
3 microscale (Fig. 6). These features, although small and not highly relevant for projectile
4 identification, emphasise the importance of understanding the dual nature of break and scar
5 formation in xenomorphic quartz that is likely to affect the formation and appearance of larger
6 features as well.

7



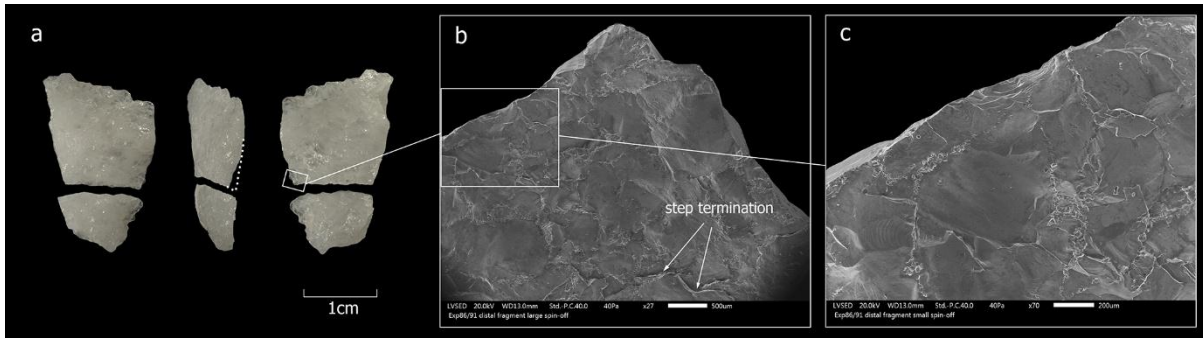
8
9

10 **Fig. 6** Spin-offs on Exp. 86/88 (xenomorphic quartz) imaged with SEM. Their initiations (A) are not obvious
11 cones, and the removals are thus more representative of cleaving than of conchoidal fracture. A shallow
12 tertiary scar (highlighted with red in the image on the right) with a well-developed cone initiation (B) and a
13 step termination (C), located at the right extremity of the spin-off, witnesses a combination of conchoidal and
14 flaw-controlled fracturing in this area. The larger of the spin-offs shows the pronounced step termination
15 already visible under low magnification. It is clearly caused by a plane of weakness intersecting the fracture
16 path, cutting the propagating crack short and resulting in a spin-off less than half a millimetre in length.
17 Original magnification 65×, scale bar 200µm

18

19 Another transverse point in xenomorphic quartz (Exp. 86/91) appears to show a combination of
20 fragmentation (*sensu* Callahan et al. 1992; Tallavaara et al. 2010) and formation of secondary
21 damage. Here, macroscopic examination of the piece shows that a significant amount of material
22 has been removed from the ventral aspect of the distal fragment of the piece that was snapped in
23 two by a non-characteristic proximal break (Fig. 7a). The termination for this supposedly large
24 removal is not visible under reflected light, nor are its outer edges. Its initiation and termination
25 could not be pinpointed with the SEM, either, but smaller removals within it could be detected (Fig.
26 7b-c). Again, it seems that a combination of different fracture phenomena is responsible for the
27 formation of these features, with fragmentation along a plane oriented roughly parallel to the
28 ventral surface being responsible for the removal of the majority of the lost volume. This kind of
29 (secondary) fragmentation is not included in the original schematic description of flake
30 fragmentation (Callahan et al. 1992; Rankama 2002; Tallavaara et al. 2010), but Tallavaara and
31 colleagues mention a number of secondary fragments that could not be refitted during the
32 experiments (Tallavaara et al. 2010). It is probable that the phenomenon described here
33 corresponds to or at least overlaps with what happens when quartz is knapped.

34

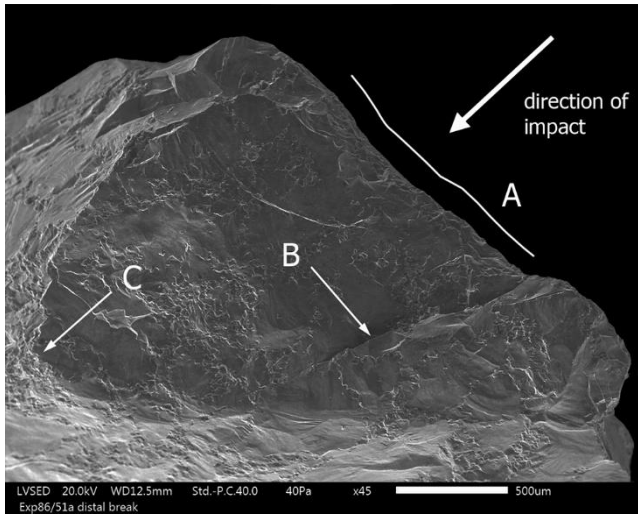


1
2
3
4
5
6
7
8
9

Fig. 7 Transverse point Exp. 86/91 (xenomorphic quartz) with a large secondary removal. a. Refitted artefact showing the loss of volume on the distal fragment. b. No clear termination for the large removal was detected in the SEM analysis, but smaller, shallow step-terminating removal without a clear point of initiation or outline is visible within it. It appears that part of the surface has split off starting from the break through a sequence of secondary removals. Original magnification 27×, scale bar 500µm. c. A small conchoidal scar with minuscule scars at its initiation, not detectable with the stereomicroscope. Original magnification 70×, scale bar 200µm

10
11
12
13
14
15
16
17
18
19

Further, a small tip break on one of the barbs made of xenomorphic quartz illustrates that while some of the features can be diffuse and hard to interpret, others can be easily misinterpreted. This break was originally classified as a bending-initiated step-terminating removal with its initiation on dorsal surface on the right side of the tip, but is in fact a snap/feather-terminating removal oriented at right angles to its originally assumed direction. What looks like a step termination is actually an irregularity on the break surface, running parallel to the direction of impact (Fig. 8). This tip break is thus another example of fracture propagation partly controlled by the existing flaws in the material, giving rise to irregular break surfaces. It shows that care is needed when interpreting small features in xenomorphic quartz.

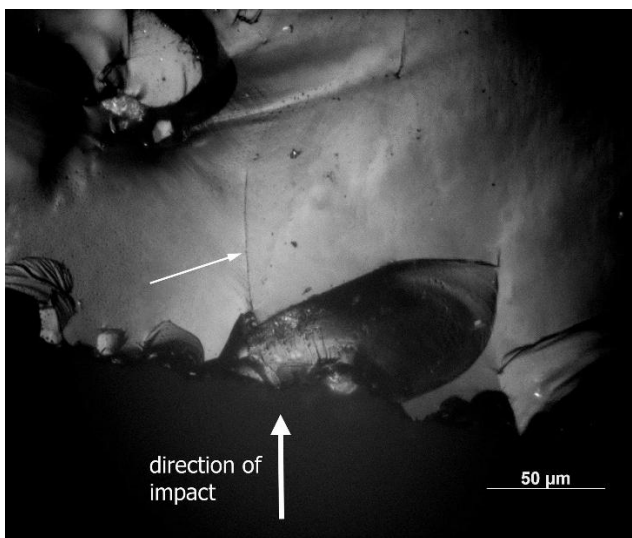


20
21
22
23
24
25
26
27
28

Fig. 8 A small tip break the type and direction of which were misidentified in the low magnification analysis. In addition to the break, crushing (A) was also observed, running perpendicular to the supposed orientation of the small break and leading to a contradictory damage pattern. The SEM image shows that the assumed step-termination (B) is in fact a structural irregularity, and the break actually reality terminates in a snap (C). Its direction is thus exactly the same as that of the crushing (small conchoidal scars) formed at its initiation. Original magnification 45×, scale bar 500µm

1 High magnification results show that some of the possibly impact-related removals were not
2 identified during low magnification analysis. While these removals are usually small, and only one
3 patch of scarring could be identified as impact damage with certainty thanks to the MLITs found in
4 association with it, these observations together suggest that the frequent use of high magnifications
5 in confirming or challenging what is seen under low magnification is a recommendable approach
6 (see also Rots and Plisson 2014; de la Peña et al. 2018).

7 While the majority of observations made in this section concern xenomorphic quartz, certain
8 recurrent features also appear in automorphic varieties. Under high magnification, projectiles in
9 both raw materials commonly show incipient cracks in the areas that came into contact with the
10 target. These cracks are dominantly oriented in the direction of impact (Fig. 9), but also several cases
11 where these longitudinal cracks occurred in combination with transverse ones were encountered.
12 The cracks thus seem to have formed as the result of compression and bending forces that occur at
13 the moment of impact. They cannot, however, be considered diagnostic of impact by themselves,
14 since similar cracks were found on fragmented bipolar flakes, usually oriented in the direction of the
15 blow.

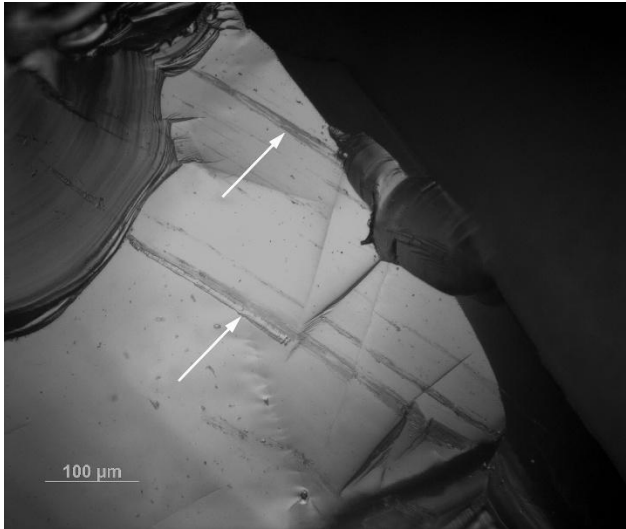


17
18
19 **Fig. 9** A crack oriented in the direction of impact (arrow), associated with small scarring. Exp. 86/57b
20 (xenomorphic quartz), original magnification 500×, scale bar 50μm

21
22 Among the linear features (MLITs) that formed on our experimental armatures upon impact,
23 different types are represented. Using Knutsson's (1988) terminology, irregular and regular striations
24 dominate heavily, whereas sleeks are extremely rare and basically only occur as one component of
25 larger features that are best characterised as very large irregular striations or abrasion tracks. This
26 suggests that the MLITs are mostly formed through brittle fracture wear and only rarely through
27 plastic deformation (see Knutsson 1988; Derndarsky and Ocklind 2001).

28 A particular type of striation occurs repeatedly in our sample. It can be characterised as an
29 unusually broad straight-sided (regular) striation. It seems to cut if not deeply, at least relatively
30 harshly into the surface, and has an even, flat bottom (Fig. 10). We interpret it as a special case of a
31 series of subsurface cracks (see Knutsson 1988; Derndarsky and Ocklind 2001). These striations occur
32 on both xenomorphic and automorphic quartz. We therefore tentatively propose that they may be
33 the result of a specific type of load situation caused when a quartz particle stuck in the target
34 scratches the surface of the projectile (cf. Kamminga 1982; Knutsson 1988).

1



2

3

4

Fig. 10 An example of broad regular MLITs described in the text. Transverse point Exp. 86/86, automorphic quartz, original magnification 200×

5

6

7

6.3 Possible sources of confusion in projectile identification

8

6.3.1 Macroscopic features

9

10

When analysing quartz, care should be taken to not confuse production-related features with impact wear. The bipolar method in particular creates breaks with pronounced secondary damage (spin-offs). These secondary scars are most pronounced in automorphic quartz, but microscopic spin-offs occur along break edges also in xenomorphic quartz, even though the majority of them are too small to be easily visible under low magnification.

11

12

13

14

Several experimental armatures in the studied sample have pronounced longitudinal breaks or removals along lateral edges (“burinations”) that were formed during production (Fig. 11a). These features may be associated with other forms of damage (e.g. abruptly terminating removals and crushing) that can also be confused with impact wear (Fig. 11b). In addition to these challenges, some pieces in automorphic quartz show more ambiguous facets that could be confused with so-called impact burinations. The latter problem is similar to erroneously identifying flakes split longitudinally during knapping as burins (*burin de siret*, Bordes 1961; for quartz, see Siiriäinen 1981). On the other hand, actual impact-related longitudinal removals along one edge can be very diffuse and almost impossible to distinguish from a break facet of a longitudinally split flake (Fig. 11c).

15

16

17

18

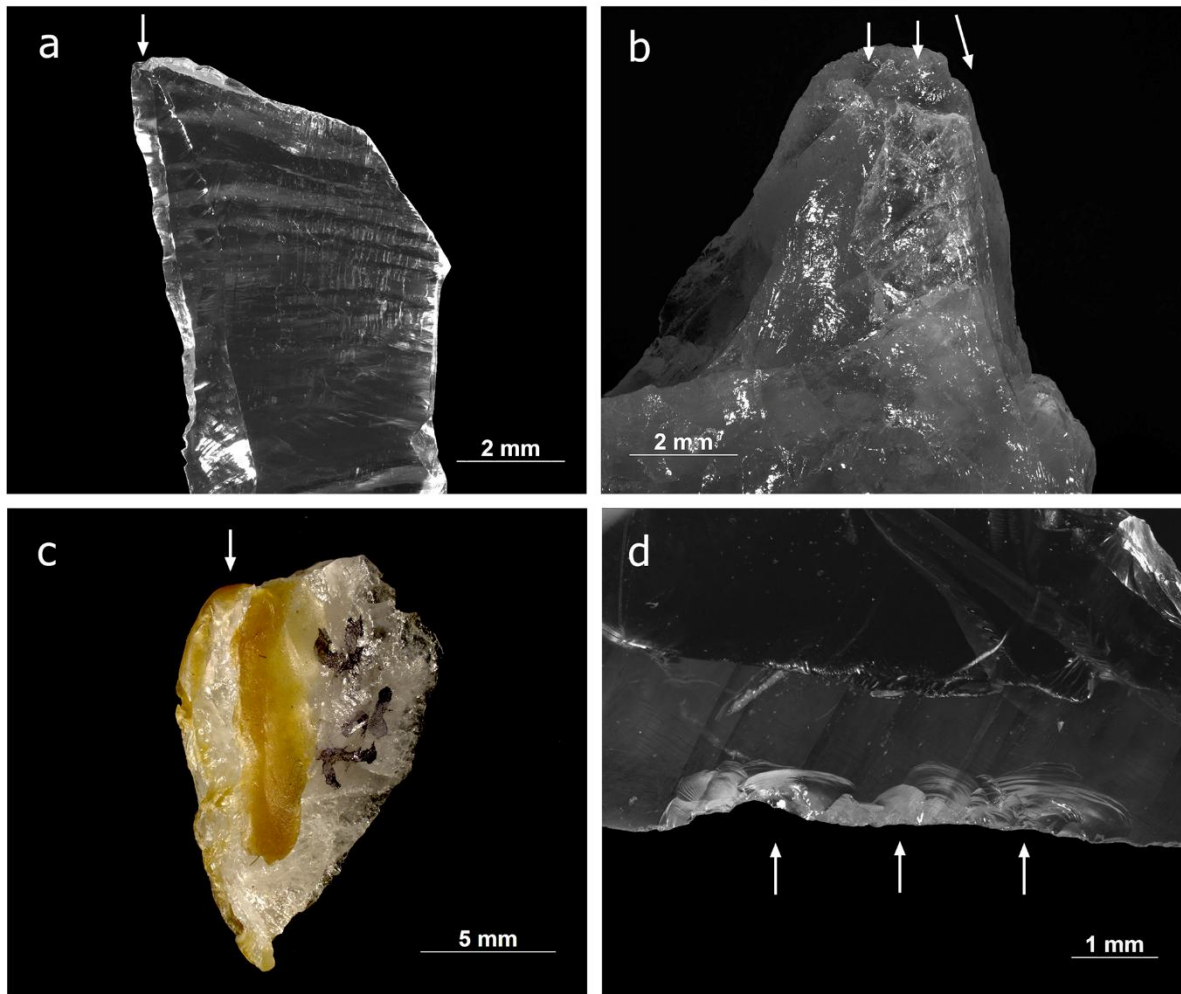
19

20

21

22

23



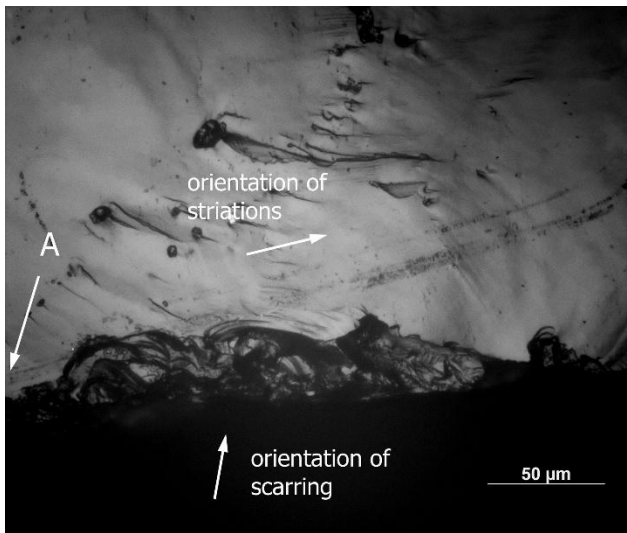
1
2
3 **Fig. 11** a. An elongated removal (“burination”) formed during knapping (flake 86/59-4 from the bipolar
4 knapping control sample, automorphic quartz, original magnification 20×) (de la Peña et al. 2018: fig 10e). b. A
5 feature resembling an impact burination associated with tip damage (step-terminating removals and crushing),
6 both resulting from knapping (Exp. 24 in Taipale 2012). Original magnification 20×. c. Example of a longitudinal
7 break (burination) on a barb. The long removal (still stuck on the shaft) was easy to detect before the removal
8 of the resin, but very difficult to tell apart from a facet formed in knapping after the piece was cleaned. d.
9 Retouch-like scarring from contact with another barb on 86/48b, automorphic quartz. Original magnification
10 32× (de la Peña et al. 2018: fig. 15b)

11
12 While production-related features can easily be confused with impact damage, impact damage can
13 in rare cases be confused with intentional retouch. This is the case with the unusually regular and
14 continuous scarring on the lateral edge of an experimental barb (Fig. 11d), caused by contact with
15 another barb upon impact. Notches form a specific case of edge damage that can sometimes result
16 from impact but also from a variety of other causes including knapping and trampling. These
17 features are discussed in detail elsewhere (de la Peña et al. 2018).

18 19 6.3.2 Microscopic features

20 The occurrence of impact-like features on freshly knapped flakes and flake fragments is a strong
21 argument for an approach that integrates low and high magnification analysis with a good
22 understanding of technological aspects of quartz industries. Our experimental sample shows that
23 MLITs form on quartz, and can in several cases help to confirm projectile function (see below).

1 A word of caution is, however, needed when it comes to identifying these features. A bipolar
 2 flake fragment from knapping experiments is an example of a case where secondary scarring
 3 associated with a break is accompanied by striations (Fig. 12). While it is possible to tell such
 4 coincidental combinations of features apart from impact traces, a much more secure approach is
 5 one that takes into account the overall morphology of the piece as well as the location and
 6 orientation of different features, and combines observations made under low and high
 7 magnifications. Linear features on quartz are frequent, and only some of them are functionally
 8 relevant.



10
 11
 12 **Fig. 12** An example of coincidental link between edge damage and striations, potentially confusable with
 13 MLITs. Here, a careful examination of the traces helps to separate them from impact wear. The striations
 14 initiate on the left side of the damaged zone (A) instead of right at the scars' edges, and the orientations of the
 15 features differ

16
 17 *6.4 Damage patterns and microscopic features on barbs*

18 Altogether four barbs were lost in the target during the experiment, and one detached from its shaft
 19 in flight before impact, and was therefore not analysed. On the remaining 40 barbs, damage is
 20 abundant, with 31 barbs showing macroscopic traces (see Table 5). Tip fractures are quite common:
 21 fourteen of the recovered barbs have breaks at their distal extremities. Five of these pieces also
 22 show a second break. One additional piece has a medial break, bringing the total number of
 23 fractured pieces to 15. Of the pieces with their tips preserved, only four show other damage on
 24 them, and when it occurs, it is generally light scarring or, in one case, crushing that is relatively
 25 subtle and difficult to characterise.

26

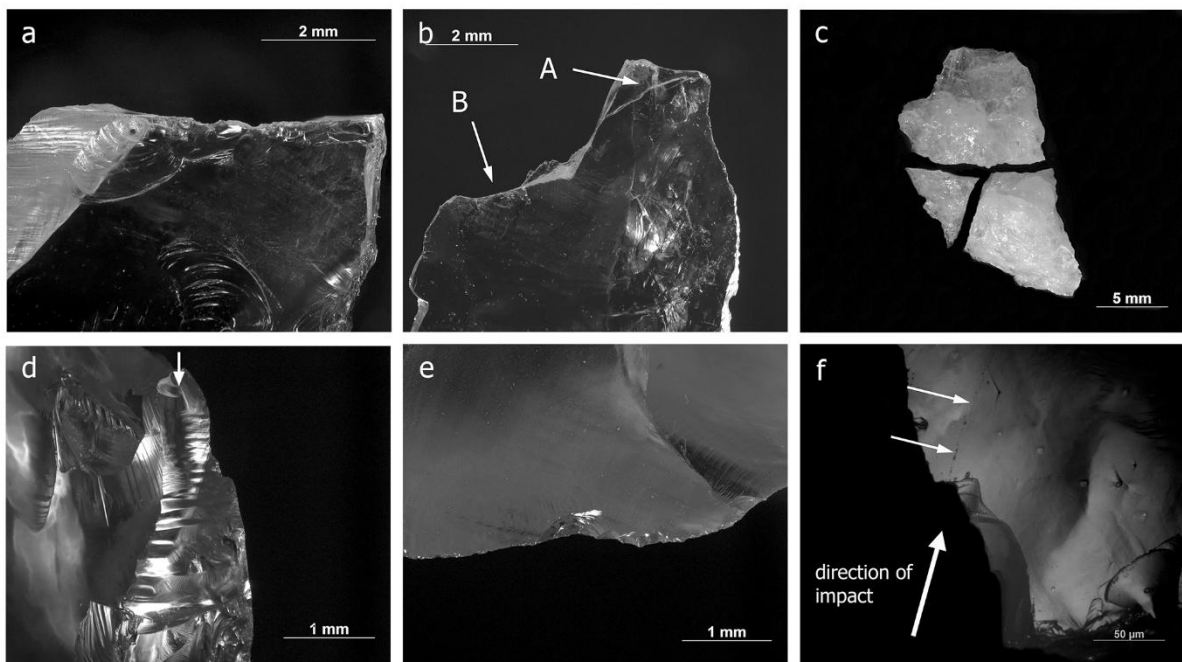
Feature type	Automorphic		Xenomorphic		Combined	
	n (N=14)	% (N=14)	n (N=26)	% (N=26)	n (N=40)	% (N=40)
Bending-initiated step-terminating surface-to-surface breaks	1	7.1%	0	0.0%	1	2.5%
Other surface-to-surface breaks	3	21.4%	8	30.8%	11	27.5%
Bending-initiated step-terminating edge-to-edge breaks	0	0.0%	0	0.0%	0	0.0%
Other edge-to-edge breaks	2	14.3%	2	7.7%	4	10.0%
Indeterminate breaks	0	0.0%	0	0.0%	0	0.0%
Several breaks on same piece	2	14.3%	3	11.5%	5	12.5%
Spin-offs	4	28.6%	1	3.8%	5	12.5%

Burinations*	3	21.4%	2	7.7%	5	12.5%
Distal scarring	1	7.1%	3	11.5%	4	10.0%
Lateral scarring (cutting edge)	13	92.9%	9	34.6%	22	55.0%
Basal scarring	3	21.4%	3	11.5%	6	15.0%
MLITs	5	35.7%	5	19.2%	10	25.0%
Other striations	6	42.9%	8	30.8%	14	35.0%
Other microwear possibly from impact	8	57.1%	18	69.2%	26	65.0%
No macroscopic damage	1	7.1%	8	30.8%	9	22.5%

1
2
3
4
5
6
7
8
9
10
11
12
13
14
15

Table 5 Frequency of different types of features on experimental quartz barbs in each raw material category and in the whole sample (for break categories, see Fig. 4). *Category “burinations” includes both longitudinal breaks and smaller removals; these features are also included in the counts in their appropriate categories (here, edge-to-edge breaks and basal scarring)

It seems that the breaks that can be considered classically diagnostic of impact, that is, the ones showing secondary scarring (spin-offs) (Fig. 13a) or a bending initiation and a step termination, are dominantly caused by the collision of two barbs, or two fragments of a single barb, against each other. This may imply that the number of diagnostic breaks on barbs increases when the hafting system allows them to detach and collide on impact. The breaks originating from contact with the target (most often skin and ballistic gel) are in general snaps, although in one case contact with skin and ballistic gel produced a complex break on the thin and fragile distal extremity of the first barb (Fig. 13b).



16
17
18
19
20
21
22
23

Fig. 13 a. Spin-offs on barb 86/48a, automorphic quartz, original magnification 32× (de la Peña et al. 2018: fig. 15c). b. A complex break at the distal extremity of barb 86/45b (automorphic quartz), showing a bending-initiated step-terminating component (A) and a snap component (B). Original magnification 25×. c. Barb 86/52a (xenomorphic quartz) exploded into three fragments through snap breaks on impact (de la Peña 2018: fig. 16a). d. Elongated removal (“burination”) on barb 86/48b (automorphic quartz), caused by counter-pressure from shaft. Original magnification 50×. e. Patch of scars forming a small notch on Exp. 86/47c

1 (automorphic quartz). Original magnification 50×. f. A MLIT associated with a microscopic burin-like removal,
2 indicating the direction of impact on 86/57a (xenomorphic quartz). Original magnification 500×
3

4 One of the barbs made of xenomorphic quartz exploded into three fragments upon impact as a
5 result of contact with skin and ballistic gel (Fig. 13c). The two breaks on this piece are clean
6 transverse and longitudinal snaps and are not accompanied with MLITs. The fragmentation of this
7 barb can be considered comparable to fragmentation of flakes during knapping (see Callahan et al.
8 1992; Tallavaara et al. 2010). While other striations were found that probably formed at the moment
9 of impact when the fragments moved against each other, these are not directly linked with the
10 break edges, are oriented in two different directions, and could easily be confused with taphonomic
11 or production-related striations if this was an archaeological piece.

12 Features traditionally termed burinations (but see Coppe and Rots 2017 for critical review of
13 the use of the term) include longitudinally or obliquely oriented breaks as well as shorter removals in
14 our sample of barbs (see Fig. 4). They seem dominantly caused by counter-pressure from the shaft
15 upon impact since they are most often located on the edge that was against the shaft (Fig. 13d).

16 Lateral scarring is the most common type of impact damage on the barbs and takes various
17 forms. Twenty-two out of 40 barbs that could be examined after the experiment show lateral edge
18 damage. Barbs coming into contact with each other on impact can cause intense edge damage, such
19 as the long stretch of retouch-like scarring observed on barb 86/48b (Fig. 11d). In most cases,
20 however, the damage is more limited and consists of small groups of scars or isolated scars. It is
21 sometimes notch-like (Fig. 13e) (de la Peña et al. 2018). The orientation of the scars is often oblique
22 to the edge and thus indicative of the position of the piece in the shaft, but also scars with a more
23 perpendicular orientation occur, making it sometimes difficult to determine the angle at which the
24 armature hit the target by looking at edge damage alone, especially in cases where the scars are few
25 in number.

26 Interestingly, considerable proportion of the lateral damage observed on the barbs (29%, or
27 15 out of 52 recorded scars or groups of scars) has been caused when they have been pressed
28 against the bindings upon impact. With the exception of two minor cone-initiated scars, all of this
29 damage is bending-initiated, whereas the scars formed through contact with the wooden shaft, the
30 target or the adhesive show both cone and bending initiations, with cone initiations dominating
31 slightly.

32 The relatively frequent detachment of barbs and their subsequent collision with each other
33 is a major cause for damage in the sample, and obscures any possible pattern in damage frequencies
34 introduced by barb position in the shaft (first, second, or third counting from the distal end of the
35 arrow). It also makes it difficult to evaluate the influence of contact material (skin, gel and/or bone)
36 on damage attributes.

37 Microscopic features on barbs consist of true MLITs (Moss 1983; Fischer et al. 1984), other
38 striations, and microscopic scarring, cracking, and abrasion. Exactly one fourth of the barbs (10/40)
39 have MLITs. Five of them are made of automorphic quartz and five of xenomorphic quartz. The
40 linear features are always parallel or slightly oblique to the cutting edge of the barb and serve as an
41 indication of the alignment of the armature with its shaft (Fig 13f).

42 The lower frequency of MLITs on xenomorphic quartz (5/26 pieces) as opposed to
43 automorphic quartz (5/14 pieces) may be partly due to observational difficulties in analysing
44 xenomorphic quartz, but more probably due to differences in the rates of edge damage formation in
45 the two raw materials. Especially the rates of lateral scarring differ greatly from one raw material to
46 the other (see Table 5). Our experimental dataset thus demonstrates the more fragile nature of
47 automorphic quartz edges, and suggests a link between the amount of macroscopic damage
48 (especially lateral scarring) and the frequency of MLITs.

1 Microwear from hafting is relatively scarce on the barbs. Twenty-five of 40 barbs showed no
2 features in their hafted portions. Of the remaining barbs, one has striations clearly formed under the
3 bindings. On several others, striations behind the rim of the hafted edge running parallel to it were
4 occasionally recorded, and one of the pieces displayed an abraded ridge. The most prominent
5 hafting-related features in our sample of barbs are thus the elongated removals (“burinations”)
6 formed by counter-pressure from the shaft, the distinctive bending-initiated scarring caused by
7 sinew bindings, and the striations formed under the bindings.

8 9 *6.5 Damage patterns and microscopic features on transverse arrowheads*

10 Three transverse points were lost during the experiment, and one of them detached from the shaft
11 before impact and was not analysed. Another point was excluded from analysis since the only
12 fragment that was recovered was too small to manipulate and could therefore not be examined in
13 detail. These pieces excluded, the sample totals 27 transverse points. Out of these, three arrows
14 either ricocheted off the skin and subsequently hit the wall behind the target, or missed the target
15 and hit the wall instead. The wall is made of autoclaved aerated concrete and is not strictly
16 comparable to materials found in nature, and cannot therefore be considered a relevant reference
17 for comparisons with archaeological material. The pieces that came into contact with it are
18 nevertheless included as a special case in the discussion of impact wear to serve as a proxy for
19 contact with hard non-animal material (stone, wood, etc.), but the microwear on them is treated
20 with caution.

21 Transverse points are characterised by breaks initiating and terminating on a surface
22 (“transverse” breaks) and breaks initiating on the cutting edge and terminating on the opposite or
23 adjacent edge (base or lateral edge; “longitudinal” breaks) (Fig. 4; Table 6). The breaks in the former
24 category are typically oblique but in some cases almost perpendicular to the direction of impact (Fig.
25 14a). The breaks in the latter category often split the piece in two almost equal parts or at least
26 removed a considerable proportion of its volume, and are oriented parallel or oblique to the axis of
27 the arrow (Fig. 4). Two of these bending-initiated breaks, one in automorphic quartz and one in
28 xenomorphic quartz, terminate in a cascade of steps (Fig. 14b), whereas the rest show snap or
29 feather terminations. In addition, one bending-initiated surface-to-surface break on an automorphic
30 quartz point has a step termination.

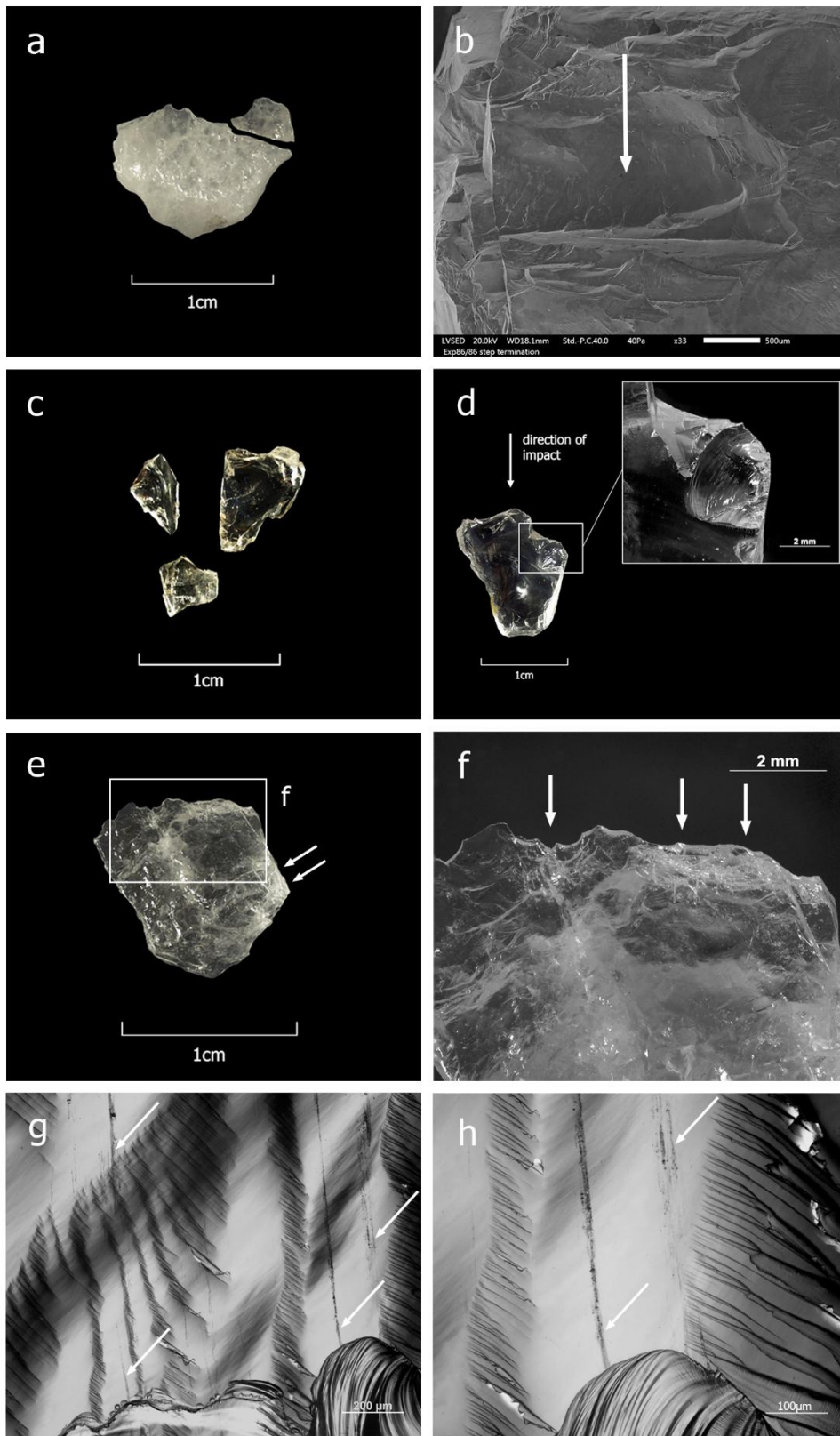
31

1
2

Feature type	Automorphic		Xenomorphic		Combined	
	n (N=11)	% (N=11)	n (N=16)	% (N=16)	n (N=27)	% (N=27)
Bending-initiated step-terminating surface-to-surface breaks	1	9.1%	0	0.0%	1	3.7%
Other surface-to-surface breaks	4	36.4%	7	43.8%	11	40.7%
Bending-initiated step-terminating edge-to-edge breaks	1	9.1%	1	6.3%	2	7.4%
Other edge-to-edge breaks	3	27.3%	1	6.3%	4	14.8%
Indeterminate breaks	0	0.0%	4	25.0%	4	14.8%
Several breaks on same piece	4	36.4%	3	18.8%	7	25.9%
Spin-offs	6	54.5%	8	50.0%	14	51.9%
Burinations*	3	27.3%	0	0.0%	3	11.1%
Distal scarring (cutting edge)	8	72.7%	8	50.0%	16	59.3%
Lateral scarring	1	9.1%	0	0.0%	1	3.7%
Basal scarring	0	0.0%	3	18.8%	3	11.1%
MLITs	8	72.7%	10	62.5%	18	66.7%
Other striations	9	81.8%	11	68.8%	20	74.1%
Other microwear possibly from impact	7	63.6%	11	68.8%	18	66.7%
No macroscopic damage	1	9.1%	1	6.3%	2	7.4%

3
4
5
6
7
8

Table 6 Frequency of different types of features on experimental quartz transverse arrowheads in each raw material category and in the whole sample (for break categories, see Fig. 4). *Category “burinations” includes both longitudinal breaks and smaller removals; these features are also included in the counts in their appropriate categories (here, edge-to-edge breaks and spin-offs)



1
2
3
4
5
6
7

Fig. 14 a. A surface-to-surface break on experimental transverse arrowhead (86/79, xenomorphic quartz), oriented almost perpendicular to the direction of impact. b. The termination of an edge-to-edge (longitudinal) break on 86/86 (xenomorphic quartz) consisting of multiple steps. The arrow indicates the general direction. Original magnification 33 \times . c. Fragmented transverse point (86/85) in automorphic quartz. d. A longitudinal fracture interrupted by zones of weakness in the material on 86/63, associated with another longitudinal break

1 that has large transverse spin-offs (shown in detail, 25×) and characteristic perpendicular damage on the
2 cutting edge. e. Perpendicular damage on the cutting edge (see also f.) and a longitudinal (oblique) break
3 associated with transverse step-terminating spin-offs (arrows) on 86/86. f. A detail of the typical perpendicular
4 damage on the cutting edge of 86/86 (see also e.). Original magnification 25×. g. MLITs associated with the
5 distal edge damage (visible in the lower part of the image) on 86/64 (automorphic quartz). Original
6 magnification 100×. h. A detail of MLITs shown in g. Original magnification 200×

7
8 Two pieces serve as examples of high-degree fragmentation. The first one, a ricochet, exploded into
9 several fragments (Fig 14c) through at least one transverse and two longitudinal breaks. The middle
10 fragment shows a complex fragmentation pattern with heavy secondary scarring, and is therefore
11 suggestive of projectile use, but its original orientation in the shaft cannot be reconstructed, and two
12 small fragments that were recovered cannot be refitted to it. The other piece came into contact with
13 the wall, and also shows a complex fragmentation pattern with two breaks initiating from the distal
14 (cutting) edge. One of the breaks has an angular path (Fig. 14d), caused by the propagation of a
15 longitudinal fracture interrupted by transversal cracks in the material. The breaks are both snap-
16 terminated, but are associated with spin-offs (Fig. 14d). This piece illustrates the brittle and partly
17 erratic behaviour of automorphic quartz on impact with hard material.

18 While some of the breaks on the transverse points are very characteristic, many others are
19 not informative from the point of view of projectile identification. Altogether four transverse breaks
20 and one longitudinal break, occurring on four pieces, cannot be characterised in detail since there
21 are no features that would allow determining where the fracture initiates and terminates. On two
22 out of these four pieces, however, other features such as spin-offs and MLITs permit identifying
23 them as projectiles and reconstructing their orientation in the shaft. This again shows that when
24 multiple scales of observation are used and the overall patterning of wear is taken into account, the
25 problem of frequent, uncharacteristic fragmentation of quartz projectiles can be partly overcome.

26 Spin-offs are relatively common on transverse points, especially when compared with barbs
27 (Tables 5 and 6, Figs 6 and 7). In addition to the general rules of spin-off formation discussed above,
28 another observation is of interest here. It concerns secondary removals associated with longitudinal,
29 obliquely oriented breaks. They occur on three fragmentary points. The secondary scars are oriented
30 perpendicular to the break's edge, and thus also (roughly) perpendicular to the direction of impact
31 (Figs 14d and 14e). From the point of view of correctly identifying the armature's orientation in the
32 shaft, these features can be potentially confusing if the overall pattern is not taken into
33 consideration. In the case of 86/86, the break's initiation on the cutting edge is associated with
34 heavy scarring in the direction of impact, and also MLITs roughly perpendicular to the cutting edge
35 can be found under high magnification (Fig. 10). These features confirm that the armature was
36 hafted transversally. Armature 86/63 shows a similar combination of distal edge damage (although
37 lighter than on 86/86) and MLITs.

38 Scarring on the cutting edges of the transverse points is systematically heavier than the
39 damage found on barbs, and only two of the transverse points do not show any macroscopic
40 scarring or other damage (Table 6). The most distinct damage pattern observed in our sample is a
41 patch of bending-initiated, invasive, large scars with abrupt or fissured terminations easily visible to
42 the naked eye, sometimes associated with a longitudinal break and/or heavy crushing and cracking
43 (Fig. 14f). The orientation of the scars is clearly perpendicular to the cutting edge of the transverse
44 point.

45 Despite the difference in armature morphologies, this damage pattern bears close
46 resemblance to that reported by Fischer et al. on flint transverse points (Fischer et al. 1984: fig. 15b-
47 c) and by Tomasso and Rots on transversally hafted flint trapezes (Tomasso et al. 2015). The brittle
48 nature of quartz contributes to the additional crushing and cracking of the point's cutting edge.

1 While this type of damage is more frequent in automorphic quartz, a similar pattern can also be seen
2 in xenomorphic quartz. The orientation of the microscopic linear features – both true MLITs and
3 striations without an obvious connection to the impact damage – leave little doubt about the
4 direction of impact (Fig 14g-h).

5 Our experiments are not comparable to those of Pargeter et al. (2016) due to obvious
6 differences in the setup (type of bow, shooting distance, their use of a target with no skin and their
7 use of commercial glue in hafting). It is, however, interesting to note here that the bending-initiated
8 breaks and large removals initiating from one surface at the cutting edge (Pargeter et al. 2016) are
9 completely absent in our sample. Two pieces in automorphic (rose) quartz from Seppä's (1995)
10 study, however, show large bending-initiated removals with complex terminations, and one of these
11 also has large spin-offs on the dorsal aspect of both fragments. One of the arrows was shot into
12 paraffin and one into the animal target, suggesting that the type of target alone does not explain the
13 difference between our and Pargeter's data. The bows between our study and Seppä's do not differ
14 significantly (47 vs 51 pounds), so the cause for the different results probably lies in artefact raw
15 material and morphology. In the rest of the sample from Seppä's study, the damage patterns fit well
16 with those in our experimental sample. This suggests that minor differences in armature design (e.g.
17 edge alignment) do not significantly increase variability in damage patterns.

18 With the exception of the extensive diffuse "spin-off" on 86/91 described earlier (Fig. 7), no
19 large spin-offs comparable to those reported by Pargeter et al. (2016) were encountered. Instead,
20 majority of the breaks recorded in our sample are transverse and longitudinal snaps, and the spin-
21 offs are usually very small in size, measuring only around 1mm. The clearest overlap between our
22 sample and that of Pargeter et al.'s are longitudinal breaks initiating on the cutting edge ("impact
23 burinations", Pargeter et al. 2016).

24 Hafting wear is not particularly common on transverse points, but the proportion of pieces
25 with definite hafting wear is still clearly higher than among the barbs. Five out of 27 transverse
26 points show traces obviously formed within the shaft. These include striations linked with edge
27 damage and other striations caused by contact with the shaft, striations associated with damaged
28 ridges, and, on one piece, basal damage associated with incipient cracks in the direction of impact.
29 Of special interest here is Exp. 86/66 which shows an oblique dorsally initiated snap exactly along
30 the haft limit. Under high magnification, the fragment that was inside the shaft shows a somewhat
31 messy pattern of striations, part of which qualify as MLITs, with two main orientations, one parallel
32 and one perpendicular to the edge of the break. A further three pieces show more ambiguous
33 striations for which other origin (production) cannot be excluded.

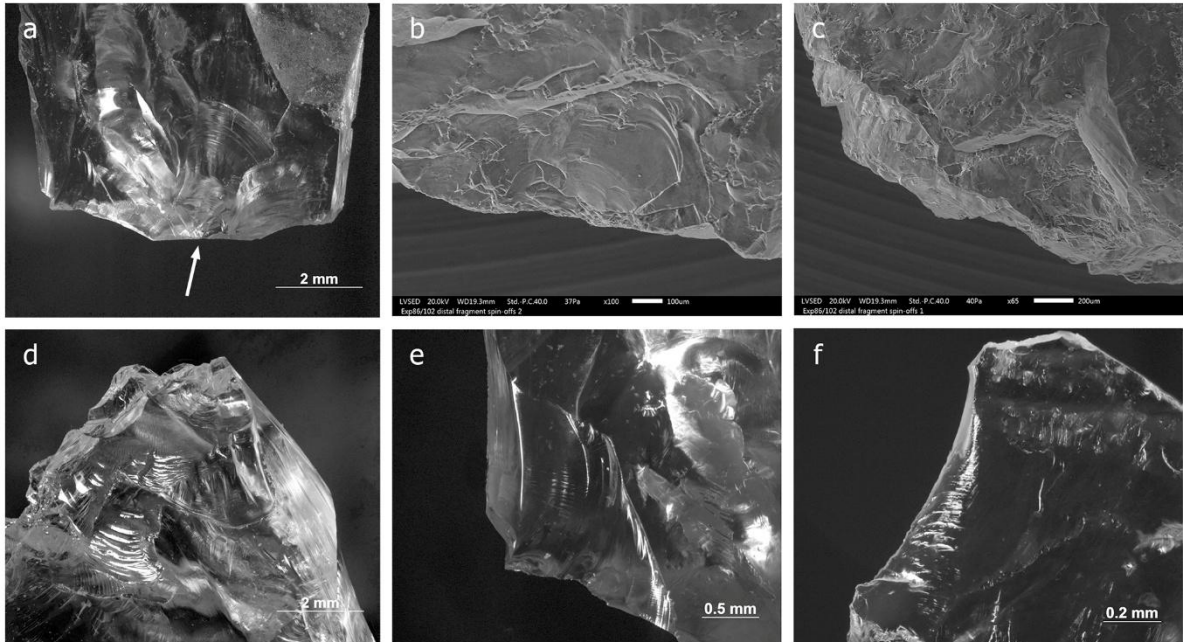
34 35 *6.6 Damage patterns and microscopic features on tips*

36 The current small sample of unmodified and minimally retouched convergent flakes hafted as tips
37 does not by any means give a comprehensive view of impact damage on this armature type. It does,
38 however, suggest certain trends that may be interesting to test through further experimentation.

39 One tip was lost during the experiment, leaving nine for analysis. Two of them show a break
40 at the tip. Both breaks, one in xenomorphic quartz and one in automorphic quartz, initiated from a
41 surface and propagated along cracks or other fragile zones in the material, and their appearance is
42 thus more characteristic of the flaw patterns in the quartz than specific forces at play during
43 breakage. One of them is associated with a second, longitudinal step-terminating break.

44 The other breaks (n=6) are typically bending-initiated snaps, in most cases clearly initiated
45 and terminated on a surface but lacking clear features that would allow determining the direction.
46 While the breaks themselves in this sample are undistinctive, four of them (three in automorphic
47 and one in xenomorphic quartz) have spin-offs, two of them on both surfaces. On automorphic
48 quartz these secondary scars can be relatively large (2–3mm; Fig. 15a), while on xenomorphic quartz

1 they are again very small, measuring less than 1mm. A further two xenomorphic quartz points have
2 possible step-terminating spin-offs that under low magnification are roughly comparable to the ones
3 documented on 86/88 (Fig. 6). Ventral spin-offs on one piece were imaged with SEM. Part of them
4 are clearly conchoidal scars (Fig. 15b) while the others, located at the opposite end of the fragment,
5 seem to be the result of the removal of microscopic blocks of quartz through cleaving (Fig. 15c).
6



7
8
9 **Fig. 15** a. Spin-offs on tip 86/95, automorphic quartz. Original magnification 25×. b. Small spin-offs with cone
10 initiations on 86/102 (xenomorphic quartz). Original magnification 100×, scale bar 100μm. c. Small spin-offs
11 without distinct initiations on 86/102 (xenomorphic quartz), formed through the removal of microscopic
12 blocks of quartz probably through cleaving. Original magnification 65×, scale bar 200μm. d. Dominantly step-
13 terminating invasive scars, with their initiations largely removed by crushing, on ventral surface of the tip of
14 86/97 (automorphic quartz). These are associated with a large step-terminating scar on the dorsal side.
15 Original magnification 25×. e. A lateral scar on tip 86/95 (automorphic quartz). Original magnification 63×. f. A
16 lateral scar on barb 86/48 (automorphic quartz). Original magnification 160×
17

18 In purely qualitative terms, spin-offs on the tips seem somewhat more pronounced and easier to
19 identify than those on transverse points and barbs. The block-like removals on 86/102 suggest that
20 this is not solely a question of the quality of the raw material in this sample, and can thus perhaps be
21 attributed to the fact that unlike on transverse points (where breaks are often oblique), the spin-offs
22 here are formed exactly in the direction of impact, leading on average to longer and deeper, and
23 also more numerous, scars (see Table 7).
24

1

Feature type	Automorphic	Xenomorphic	Combined
	n (N=4)	n (N=5)	n (N=9)
Bending-initiated step-terminating surface-to-surface breaks	0	0	0
Other surface-to-surface breaks	2	2	4
Bending-initiated step-terminating edge-to-edge breaks	0	1	1
Other edge-to-edge breaks	0	1	1
Indeterminate breaks	0	3	3
Several breaks on same piece	0	2	2
Spin-offs	3	3	6
Burinations*	0	2	2
Distal scarring (cutting edge)	2	0	2
Lateral scarring	3	2	5
Basal scarring	2	1	3
MLITs	2	1	3
Other striations	3	2	5
Other microwear possibly from impact	3	3	6
No macroscopic damage	0	1	1

2

3 **Table 7** Frequency of different types of features on experimental quartz tips in each raw material category and
4 in the whole sample. *Category “burinations” includes here secondary removals that are also counted in spin-
5 offs

6

7 Tip damage is rare in this sample, but when it occurs, it can be extreme (Fig. 15d). What is of special
8 interest here is lateral damage that is both frequent and partly similar to that observed on barbs.
9 However, even though the characteristics of lateral scarring on the two projectile types overlap, with
10 both showing bending-initiated, often invasive scars oriented obliquely to the edge (Fig. 15e-f), the
11 removals on the tips seem to be systematically larger. More importantly, three out of five of the
12 pieces showing lateral damage also have a break associated with spin-offs. This kind of combination
13 is rare on barbs. Even though the tip sample is small, it may well be that focusing on overall wear
14 patterns offers a key to distinguishing between these two types of projectiles.

15 MLITs occur on three of the nine tips that could be analysed, in two cases associated with a
16 break and in one case associated with the heavy distal damage mentioned above. Hafting wear is
17 practically absent in this sample. Only one piece (86/100) shows tentative wear in the form of
18 microscopic abrasion and cracking on its ventral proximal corner.

19

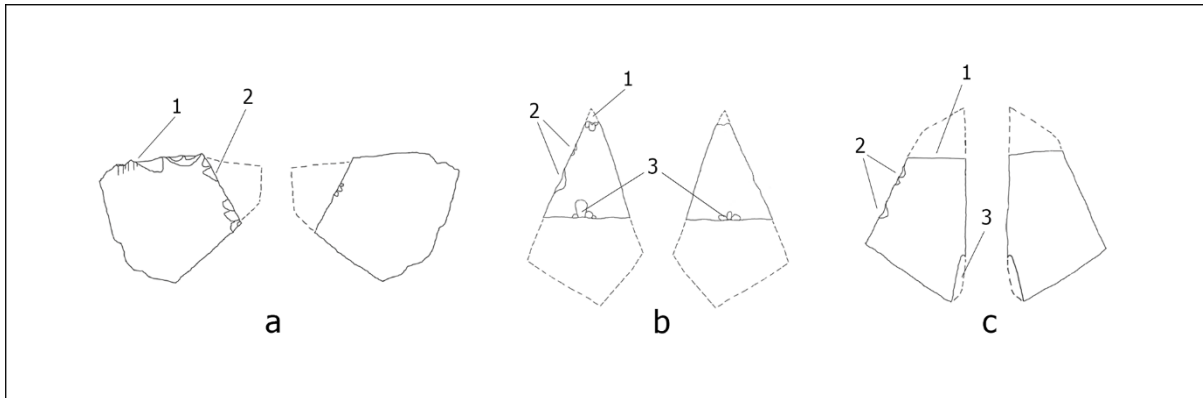
20 7 Discussion

21

22 *7.1 Do wear patterns allow the identification of barbs, transverse points and convergent* 23 *points?*

24 In sum, even though the majority of breaks in all projectile categories are not suggestive of impact,
25 and their number is probably increased by the fracturing of xenomorphic quartz along internal
26 discontinuities, impurities and other flaws, certain repetitive patterns seem to emerge that could
27 allow reconstructing the orientation of the armature in its shaft on the condition that the number of
28 damaged pieces in the sample is sufficiently high. In each case, the overall patterning of traces is the
29 key, and any analysis attempting to make these kinds of distinctions should focus on combinations of
30 features instead of searching for one specific trait (see Rots and Plisson 2014; Rots 2016).

1 The wear on transverse points is clearly distinct from that on the other two armature types.
 2 Features that are limited to this category include invasive bending-initiated abruptly terminating
 3 damage oriented perpendicular to the cutting edge (often accompanied by MLITs), bending-initiated
 4 step-terminating longitudinal breaks initiated from the cutting edge, and oblique breaks associated
 5 with spin-offs oriented roughly perpendicular to the direction of impact (Fig. 16a). While for
 6 Mesolithic transverse points, the morphology is often by itself enough to determine the hafting
 7 orientation, this is not necessarily the case for all morphologies (for competing hypotheses on
 8 Howiesons Poort segments, see e.g. Lombard 2011; de la Peña et al. 2018), in which case these
 9 criteria can help to distinguish between lateral and transverse hafting.



11 **Fig. 16** Idealised drawings of typical wear patterns on different projectile types. a. Transverse points. 1:
 12 invasive bending-initiated abruptly terminating edge damage associated with MLITs, 2: oblique break
 13 associated with perpendicular spin-offs. b. Convergent tips. 1: scarring responsible for the removal of the
 14 outermost tip, 2: lateral obliquely or perpendicularly oriented damage, 3: break with spin-offs. c. Barbs. 1: tip
 15 break (in the experimental sample, typically a non-characteristic snap), 2: lateral obliquely or perpendicularly
 16 oriented damage, 3: an elongated removal on the non-active edge caused by counter-pressure from the shaft
 17
 18
 19

20 Convergent tips and barbs share certain features such as bending-initiated lateral scarring oriented
 21 obliquely to the edge (Fig. 16b-c: 2). It is obvious that the chances of reliably telling apart these two
 22 armature types can only be evaluated through further experimentation involving tips. Yet, the small
 23 sample examined here allows the formulation of preliminary hypotheses about potentially useful
 24 criteria for identifying convergent points archaeologically.

25 While the breaks on tips are typically as undiagnostic as in the other two groups, spin-offs
 26 are more frequent and easily identifiable than on barbs and transverse points, not least because tips
 27 are the only category that recurrently shows bifacial spin-offs. The contrast with barbs is particularly
 28 clear. Also heavy distal damage (Fig. 16b: 1) is absent on barbs, although it has to be noted that it is
 29 not extremely frequent on tips, either.

30 Table 8 shows the proportion of experimental pieces with convincing evidence of projectile
 31 use within each raw material category and projectile type. Here, macroscopic and microscopic
 32 evidence were combined, and strict criteria were applied. Only armatures that showed a
 33 combination of impact damage and MLITs or a combination of macroscopic features indicative of
 34 projectile use are included in the counts. When the tip sample, which is too small for meaningful
 35 comparisons, is excluded, the identification rate is highest for transverse points, and lowest for barbs
 36 in xenomorphic quartz. A breakdown of MLITs per projectile and feature type (Table 9) offers an
 37 explanation: linear impact features are particularly frequently associated with distal damage on
 38 transverse points.

	Automorphic quartz			Xenomorphic quartz		
	certain	total	% certain	certain	total	% certain
Barbs	5	14	35.7%	4	26	15.4%
Transverse	7	13	53.8%	8	16	50.0%
Tips	3	4	75.0%	1	5	20.0%

1 **Table 8** Number of pieces showing convincing evidence of projectile use (a combination of impact damage and
2 MLITs or a combination of macroscopic features) in the experimental samples, divided by raw material and
3 projectile type. These numbers represent pieces that could be confidently identified as projectiles in an
4 archaeological setting
5

Feature type	Barbs				Transverse				Tips			
	MLITs			Total	MLITs			Total	MLITs			Total
	yes	no	NA		yes	no	NA		yes	no	NA	
Bending-in. step-term. surface-to-surface breaks	2	0	0	2	0	1	0	1	0	0	0	0
Other surface-to-surface breaks	2	9	0	11	4	7	0	12	2	1	1	4
Edge-to-edge breaks (incl. burinations)	0	3	1	5	3	3	0	6	0	1	0	1
Indeterminate breaks	0	0	0	0	2	2	0	4	0	3	0	3
Spin-offs	0	3	1	3	3	11	0	14	2	4	0	6
Distal damage	0	4	0	4	10	5	1	16	1	0	1	2
Lateral damage	4	18	0	22	0	1	0	1	0	4	1	5
Basal damage	0	6	0	6	0	3	0	3	0	3	0	3
No macroscopic damage	0	9	0	9	1	1	0	2	0	1	0	1

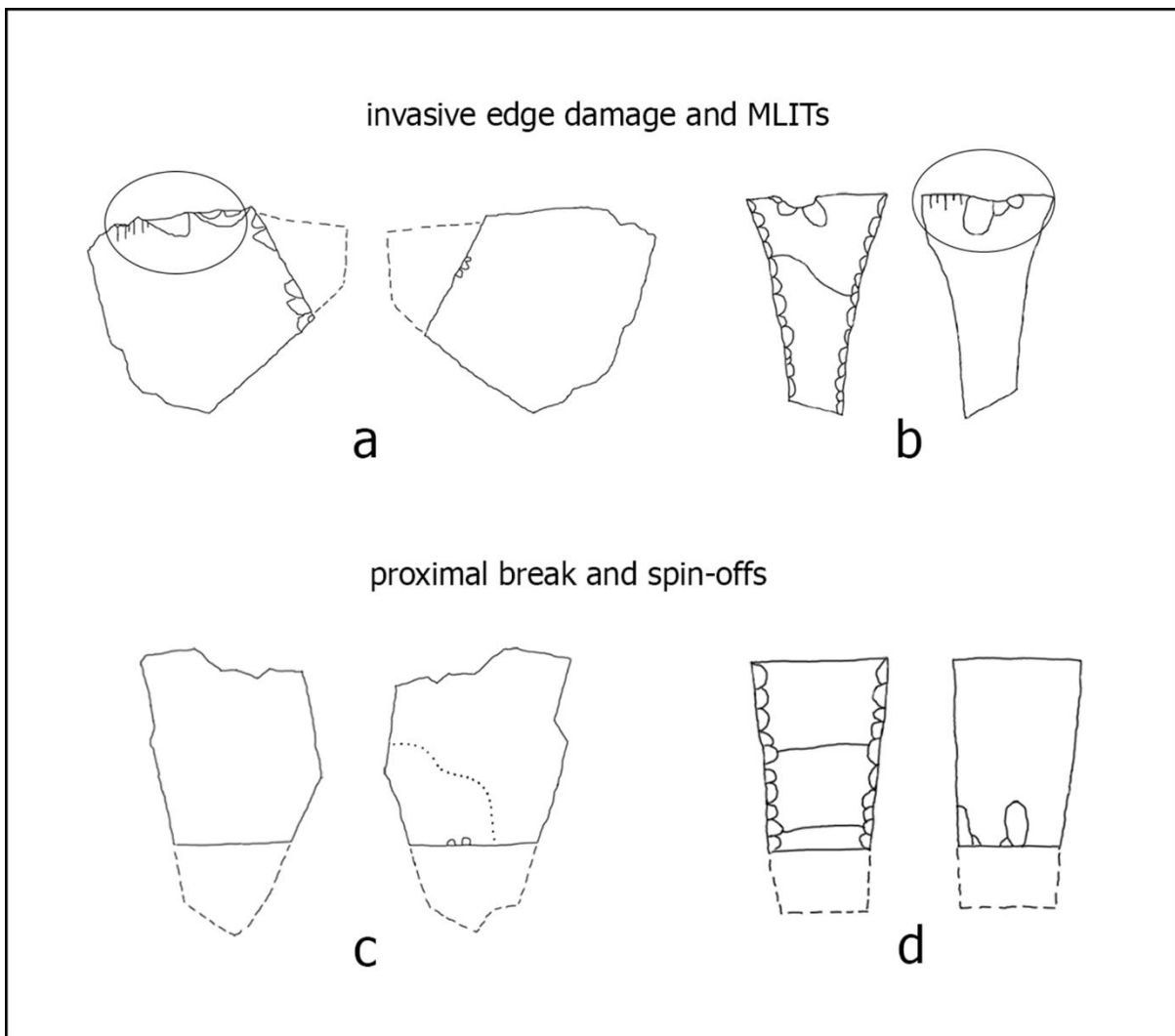
6 **Table 9** Occurrence of MLITs (microscopic linear impact traces) in association with different types of impact
7 features in the experimental sample. Distal damage refers to damage on the distal tip for convergent tips and
8 barbs, and damage on the cutting edge for transverse points
9

10 These results suggest that the archaeological visibility of quartz barbs in general, and barbs in
11 xenomorphic quartz in particular, may be low in comparison to other armature types. They have,
12 however, been recently identified in different archaeological contexts (Knutsson et al. 2015a; de la
13 Peña et al. 2018), which suggests that this problem can be partly overcome with a techno-functional
14 approach and appropriate sampling strategies.
15

16 7.2 Quartz and flint

17 When our barb data are compared to the results of a recent study that involved flint barbs (Rots
18 2016), certain similarities and differences emerge. Tip breaks on flint barbs in Rots's study are rarely
19 step-terminating, which is also the case for both of our raw material samples, where the only step-
20 terminating break (on automorphic quartz) occurred as the result of barb collision. It is clear that the
21 proportion of automorphic quartz pieces with lateral edge damage (92.9%; Table 5) is in the same
22 range with that of flint barbs, all of which showed lateral scarring of some type (calculated from
23 Rots, 2016, table 12.3), while the frequency of lateral damage is considerably lower in xenomorphic
24 quartz (34.6%; Table 45). This suggests that while general patterns of damage formation within a
25 projectile type may overlap between flint and quartz, certain qualities of xenomorphic quartz will
26 introduce variability that can lead to lower success rates in projectile identification.

1 Our transverse points show damage patterns that are partly similar to those documented in
 2 previous studies on flint (Fig. 16a; Fischer et al. 1984; Tomasso et al. 2015). In addition to the
 3 invasive scarring on cutting edge (Fig. 17a-b and 14f, Fischer et al. 1984: fig. 15b-c), the point
 4 discussed in the context of unusual spin-offs (Fig. 7) is relevant here because it is morphologically
 5 roughly similar to the points used by Fischer and colleagues. It shows a proximal break like the point
 6 depicted by Fischer et al. (1984). The difference is in the quality of the ventral “spin-offs” on the
 7 distal fragment: our point shows a combination of fragmentation (cleaving) and minuscule
 8 conchoidal scars (Figs 17c-d). This illustrates that while there are indications that some damage
 9 patterns are analogous on flint and quartz, they can become difficult to detect due to the
 10 idiosyncratic behaviour of the less homogenous raw material. This example also warns against the
 11 use of spin-off measurements as diagnostic criteria without a careful consideration of the effect of
 12 raw material properties.
 13



14
 15
 16 **Fig. 17** Idealised drawings of wear patterns on quartz transverse points (a, c) and flint transverse points as
 17 described by Fischer et al. (b, d; Fischer et al. 1984: figs 7H and 15). a. Invasive distal scarring oriented
 18 perpendicularly to the cutting edge and associated with MLITs. b. Similar pattern in flint depicted by Fischer et
 19 al. (redrawn from Fischer et al. 1984: fig. 15). c. Wear pattern involving a proximal transverse break and spin-
 20 offs (see also Fig. 6). d. Similar damage on flint transverse point (redrawn from Fischer et al. 1984: fig. 7H)
 21

1 The applicability of the criteria used for identifying projectiles made of flint and other
2 cryptocrystalline rocks is a complicated matter. Our preliminary identification of certain similarities
3 in the patterning of wear between the two different raw materials seems to speak for Pargeter's
4 (2013) argument that rock type variability is secondary in comparison to tool use in macrofracture
5 formation. Patterns similar to flint *do* exist even in xenomorphic quartz. These patterns are,
6 however, infrequent and often ambiguous. We are therefore not convinced that the relationship
7 between tool use and raw material properties is straightforwardly hierarchical. The frequency of
8 partly or fully flaw-controlled breaks in all projectile categories suggests that the variability in
9 structural properties both between and within different types of quartz is enormous. For this reason,
10 we believe that only rigorous large-scale experimentation – preferably combined with mechanical
11 testing of raw material samples (de Lombera-Hermida and Rodríguez-Rellán 2016; Rodríguez-Rellán
12 2016) and appropriate quantification of impact features – will allow determining to what extent
13 internal planes and flaws in quartz interfere with the formation of diagnostic wear patterns. Until
14 then, uncritical application of descriptive and analytical criteria developed for flint should preferably
15 be avoided in the analysis of quartz projectiles.

16

17 *7.3 Quartz and impact damage quantification*

18 We believe that before methods based on quantification of wear features, such as measuring the
19 size (area) of impact-related removals (Pargeter et al. 2016), can be successfully applied, the
20 idiosyncratic behaviour of quartz under mechanical stress needs to be well understood and the rules
21 applied to the specific case of impact fracture formation. In our view, this requires further,
22 controlled experimentation involving large samples, statistical analysis, and ideally collaboration
23 with experts from other relevant disciplines such as geology.

24 Based on our current dataset, we suggest that the length of impact fracture propagation and
25 the volume of removals in xenomorphic quartz and in more erratic forms of automorphic quartz are
26 controlled not only by the properties of the weapon and the target (point morphology, kinetic
27 energy, angle of impact, resistance of the target) but also, and to a significant extent, by the
28 presence and severeness of internal planes, impurities, and other zones of weakness in the lithic
29 armature.

30 It seems evident that this variability in raw material qualities does not prevent the formation
31 of impact breaks considered classically diagnostic (compare Pargeter et al. 2016). It leads, however,
32 into the formation of a myriad of more subtle and ambiguous features that will keep the proportion
33 of easily identifiable impact breaks low in comparison to cryptocrystalline rocks. It will also introduce
34 additional variability into the dimensions and other characteristics of the more pronounced features.
35 The ambiguous spin-offs documented with the SEM demonstrate the effects of the co-existence of
36 conchoidal fracture and breakage along cleavage planes and other irregularities in xenomorphic
37 quartz. As a result, most of the spin-offs are either fully formed but microscopic conchoidal scars, or
38 removals with diffuse initiations cut short by flaws in the material. In both cases, they often measure
39 less than 1mm in length, which has clear implications for approaches that search for sizeable,
40 “diagnostic” spin-offs.

41 These observations call for a methodology that not only acknowledges but also, where
42 possible, takes advantage of the particular behaviour of quartz under mechanical stress.

43

44 *7.4 Can variables other than raw material be responsible for the observed patterns?*

45 Our experimental material shows a relatively low frequency of easily identifiable impact breaks and
46 several examples of cases where impact-related features are either small in size (e.g. microscopic
47 spin-offs) or unusual in terms of initiation, propagation and termination when compared to
48 cryptocrystalline rocks. We have argued that these characteristics are the result of particular

1 mechanical properties of quartz that affect fracture formation during projectile impact. An
2 alternative explanation for the observed traits in the experimental sample could, however, lie in the
3 experimental design. The main variables that could affect the frequency and characteristics of
4 macroscopic impact damage are the robustness of the hafting system and armature morphology.

5 The strength of the hafting arrangement has an influence on breakage patterns in lithic
6 armatures since the weakest element in the projectile (or target) will suffer damage unless the
7 projectile's energy is dissipated through elastic deformation of the target (Plisson and Beyries, 1998;
8 Rots and Plisson, 2014). This means that a failing hafting system will reduce the amount of damage
9 to the lithic component of the projectile by absorbing a significant part of the energy. A brief
10 examination of the cases where the hafting failed (i.e., the armature detached or moved
11 considerably in its shaft) allows evaluating whether one or several of the bonding systems used
12 (sinew, adhesive, and a combination of the two) produced considerable failure rates that would
13 affect the wear patterns and the interpretation of the effects of the properties of the quartz itself on
14 impact damage formation.

15 Given that the barbs were hafted in sets of three, hafting failure actually increases the
16 frequency of impact breaks for this group of armatures by increasing the chances of contact with
17 hard material (another barb) (see section 6.4). Barbs therefore form a special case and are not
18 considered here. When the remaining projectiles (transverse and convergent tips) are examined,
19 there are altogether four projectiles where the armature detached or considerably moved within its
20 shaft without piercing the skin (see Tables 2–4). These can be considered the cases where there is
21 most reason to suspect that the hafting system was not resistant enough to allow the formation of
22 clear impact traces on the lithic armature. They include one convergent tip hafted with adhesive,
23 and two transverse points hafted with sinew and adhesive. One of the transverse armatures shows a
24 longitudinal break, spin-offs, and distal edge damage, and the other shows distal and basal edge
25 damage. The convergent tip is the only one of the three that does not display macroscopic damage.

26 In addition to these three arrows, there are 11 cases where the armature de-hafted either
27 inside the target on impact or when removing the projectile from the target. Of these, four show a
28 break, five show edge damage of varying sorts, and only two show no macroscopic damage at all.

29 These counts indicate that while hafting failure may affect the observed rate of breakage,
30 the matter is not straightforward since some of the most obvious impact breaks actually occur in
31 these two groups due to the fact that some of the armatures came into contact with hard material.
32 The cases where the hafting "failed" are spread over all three types of bonding systems used. This
33 suggests that rather than being simply a question of the raw materials chosen (sinew, adhesive), the
34 robustness of the hafting arrangement is affected also by other factors such as for example
35 armature size and morphology and the amount and location of bindings and/or glue applied. Our
36 current dataset is too varied to allow an accurate evaluation of the combined effect of the hafting
37 arrangement and the contact material(s), and a thorough evaluation of the role of the former would
38 require a different (more controlled) setup. For the purposes of the present study, however, it
39 suffices to say that there is no simple relationship between the robustness of the hafting
40 arrangement and the amount or quality of impact damage formed. This means that the patterns we
41 observe are not significantly affected by failures in hafting.

42 Armature morphology is a complex variable that cannot be reduced to simple measures of
43 length, width or thickness since other characteristics such as edge angles and surface convexities are
44 crucial for fracture formation. While we acknowledge that the experimental samples are varied with
45 respect to morphology due to the low amount of retouch and the subsequently low degree of
46 standardisation, we assume that the variation that armature morphology introduces into the
47 observed breakage patterns is mostly random and does not result in systematic biases. We therefore
48 consider that the patterns we have described are representative of the behaviour of quartz on
49 impact. It is clear, however, that future experiments that aim at a more detailed registration and

1 interpretation of impact fracture phenomena should be structured so that the effect of each variable
2 is controlled for and tested using larger samples.

3 4 *7.5 Impact damage on automorphic vs xenomorphic quartz*

5 When the automorphic quartz armatures in our samples are viewed side by side with their
6 xenomorphic counterparts, it is clear that features are usually much easier to identify and
7 characterise on the former, and that it shows a higher frequency of diagnostic combinations of
8 features. While our samples are too small and varied for evaluating how rare these patterns are in
9 xenomorphic quartz, their presence among a relatively limited number of experimental armatures
10 seems to suggest that when samples (assemblages) are large enough, such patterns should emerge
11 even if they are partly prohibited by the unpredictable behaviour of xenomorphic quartz.

12 Furthermore, a “blind” division of the sample into automorphic quartz and xenomorphic quartz is
13 not necessarily the best strategy when the goal is to understand the details of wear formation in the
14 quartz family, as the variability within each group can be quite large (de Lombera Hermida 2009;
15 Tardy et al. 2016). In our sample, the angular fracture pattern observed on one of the transverse
16 points in automorphic quartz (Fig. 14d) serves as one example of slightly erratic behaviour of this
17 raw material. While automorphic and xenomorphic varieties *typically* behave differently from one
18 another, the variability within each category is significant enough to propose that employing only a
19 simple division like this may lead into ignoring structural characteristics that can be relevant for
20 impact damage formation. Further experimental work is needed for understanding which structural
21 properties control fracture propagation and how, and whether or not they are visible to the naked
22 eye.

23 8 Conclusions

24 Our data supports the hypothesis that the mineralogical properties of quartz, as described in recent
25 archaeological literature, affect impact damage formation. These properties result in breakage along
26 fault planes and other zones of weakness, in removals with irregular or diffuse morphologies, and in
27 the interruption of fracture propagation.

28 While breaks and damage generally considered as “diagnostic” of impact in flint armatures
29 also occur in quartz, they seem to be less frequent. Further work is needed to understand their
30 relevance for projectile identification and interpretation. In addition to traits considered classically
31 “diagnostic”, we documented a number of more ambiguous features that seem to be the
32 consequence of fully or partly flaw-controlled fracture propagation. Also the pronounced brittleness
33 of quartz contributes to the differences between quartz and flint projectiles.

34 Regardless of these effects, a number of criteria can be proposed for distinguishing among
35 quartz barbs, transversely hafted armatures, and convergent tips on an assemblage level. Barbs tend
36 to show varying combinations of lateral damage, tip breaks (typically snaps), and removals caused by
37 counter-pressure from the shaft. Transversally hafted pieces are characterised by heavy
38 perpendicularly oriented damage at the cutting edge that is often accompanied by MLITs, as well as
39 longitudinal (oblique) breaks that sometimes show spin-offs oriented perpendicularly to the
40 direction of impact. The small sample of tips suggests that while the features on them and on the
41 barbs can overlap, spin-offs are likely to be more pronounced and more frequent on tips, and heavy
42 damage on the outermost tip is also more likely to occur.

43 These results show that impact wear on quartz is a topic worth further exploration and can
44 significantly contribute to our understanding of past hunting practices. Analytical methods should,
45 however, be adjusted so that they take into consideration the particular behaviour of quartz under
46 mechanical stress. This goal is best reached by systematic large-scale experimentation, mechanical
47 testing, and an analytical strategy that combines different microscopic techniques and scales of
48 observation.

1 References

- 2
- 3 Barton RNE, Bergman CA (1982) Hunters at Hengistbury: Some evidence from experimental
4 archaeology. *World Archaeol.* <https://doi.org/10.1080/00438243.1982.9979864>
- 5 Bordes F (1961) *Typologie du Paléolithique ancien et moyen*. Delmas, Bordeaux
- 6 Broadbent ND, Knutsson K (1975) An Experimental Analysis of Quartz Scrapers. Results and
7 Applications. *Fornvännen*: 113–128
- 8 Callahan E, Forsberg L, Knutsson K, Lindgren C (1992) Frakturbilder. Kulturhistoriska kommentarer till
9 det säregna sönderfallet vid bearbetning av kvarts. *Tor* 24: 27–63.
- 10 Coppe J, Rots V (2017) Focus on the target. The importance of a transparent fracture terminology for
11 understanding projectile points and projecting modes. *J Archaeol Sci: Reports*.
12 <https://doi.org/10.1016/j.jasrep.2017.01.010>
- 13 de la Peña P, Taipale N, Wadley L, Rots V (2018) A techno-functional perspective on quartz micro-
14 notches in Sibudu’s Howiesons Poort indicates the use of barbs in hunting technology. *J*
15 *Archaeol Sci.* <https://doi.org/10.1016/j.jas.2018.03.001>
- 16 de Lombera-Hermida A, Rodríguez-Rellán C (2016) Quartzes matter. Understanding the
17 technological and behavioural complexity in quartz lithic assemblages. *Quat Int.*
18 <https://doi.org/10.1016/j.quaint.2016.11.039>
- 19 de Lombera Hermida A (2009) The scar identification of lithic quartz industries. In: Sternke F,
20 Eigeland L, Costa L-J (eds) *Non-flint Raw Material Use in Prehistory. Old Prejudices and New*
21 *Directions*, BAR International Series 1939. Archaeopress, Oxford, pp 5–12
- 22 Derndarsky M, Ocklind G (2001) Some Preliminary Observations on Subsurface Damage on
23 Experimental and Archaeological Quartz Tools using CLSM and Dye. *J Archaeol Sci.*
24 <https://doi.org/10.1006/jasc.2000.0646>
- 25 Domanski M, Webb J, Boland J (1994) Mechanical Properties of Stone Artefact Materials and the
26 Effect of Heat Treatment. *Archaeom* 36: 177–208
- 27 Driscoll K (2010) *Understanding quartz technology in early prehistoric Ireland*. Dissertation,
28 University College Dublin
- 29 Driscoll K (2011a) Vein quartz in lithic traditions: An analysis based on experimental archaeology. *J*
30 *Archaeol Sci.* <https://doi.org/10.1016/j.jas.2010.10.027>
- 31 Driscoll K (2011b) Identifying and classifying vein quartz artefacts: An experiment conducted at the
32 World Archaeological Congress, 2008. *Archaeom.* [https://doi.org/10.1111/j.1475-](https://doi.org/10.1111/j.1475-4754.2011.00600.x)
33 [4754.2011.00600.x](https://doi.org/10.1111/j.1475-4754.2011.00600.x)
- 34 Fernández-Marchena JL, Ollé A (2016) Microscopic analysis of technical and functional traces as a
35 method for the use-wear analysis of rock crystal tools. *Quat Int* 424: 171–190
- 36 Fernández-Marchena JL, Rabuñal Ramón J, Argudo-García G (2017) Experimental and functional
37 analysis of rock crystal projectiles. In: *Playing with the time. Experimental archaeology and the*
38 *study of the past*, pp 101–106
- 39 Fischer A, Vemming Hansen P, Rasmussen P (1984) Macro and micro wear traces on lithic projectile
40 points: experimental results and prehistoric examples. *J Dan Archaeol* 3: 19–46
- 41 Fullagar R (1986) Use-wear on quartz. In: Ward GK (ed) *Archaeology at ANZAAS*, Canberra. Canberra
42 Archaeological Society, Canberra, pp 191–197
- 43 Geneste JM, Plisson H (1990) Technologie fonctionnelle des pointes a cran Solutréennes: l’apport des
44 nouvelles données de la grotte de Combe Saunière (Dordogne). In: Kozłowski JK (ed) *Feuilles de*
45 *pierre. Les Industries à pointes foliacées du Paléolithique supérieur européen. Actes du*
46 *colloque international de Cracovie (1989)*. ERAUL, Liège, pp. 293–320
- 47 Kamminga J (1982) *Over the edge: functional analysis of Australian stone tools*. University of
48 Queensland
- 49 Knutsson H, Knutsson K, Molin F, Zetterlund P (2015a) From flint to quartz: Organization of lithic
50 technology in relation to raw material availability during the pioneer process of Scandinavia.
51 *Quat Int.* <https://doi.org/10.1016/j.quaint.2015.10.062>

- 1 Knutsson H, Knutsson K, Taipale N, Tallavaara M, Darmark K (2015b) How shattered flakes were
2 used: Micro-wear analysis of quartz flake fragments. *J Archaeol Sci: Reports*.
3 <https://doi.org/10.1016/j.jasrep.2015.04.008>
- 4 Knutsson K (1988) Patterns of tool use. Scanning electron microscopy of experimental quartz tools.
5 *Societas Archaeologica Upsaliensis*, Uppsala
- 6 Lindgren C (1998) Shapes of quartz and shapes of minds. In: Holm L, Knutsson K (eds) *Proceedings*
7 *from the Third Flint Alternatives Conference at Uppsala, Sweden, October 18–20, 1996*.
8 *Occasional Papers in Archaeology* 16. Department of Archaeology and Ancient History, Uppsala
9 University, Uppsala, pp. 95–103.
- 10 Lombard M (2011) Quartz-tipped arrows older than 60 ka: Further use-trace evidence from Sibudu,
11 KwaZulu-Natal, South Africa. *J Archaeol Sci*. <https://doi.org/10.1016/j.jas.2011.04.001>
- 12 Manninen MA (2016) The effect of raw material properties on flake and flake-tool dimensions: A
13 comparison between quartz and chert. *Quat Int*. <https://doi.org/10.1016/j.quaint.2015.12.096>
- 14 Manninen MA, Knutsson K (2011) Northern inland oblique point sites – a new look into the Late
15 Mesolithic oblique point tradition in Eastern Fennoscandia. In: Rankama T (ed) *Mesolithic*
16 *Interfaces. Variability in Lithic Technologies in Eastern Fennoscandia*. Monographs of the
17 Archaeological society of Finland. Archaeological Society of Finland, Saarijärvi, pp. 142–175
- 18 Manninen MA, Tallavaara M (2011) Descent history of Mesolithic oblique points in eastern
19 Fennoscandia – a technological comparison between two artefact populations. In: Rankama T
20 (ed) *Mesolithic Interfaces. Variability in Lithic Technologies in Eastern Fennoscandia*.
21 Monographs of the Archaeological society of Finland. Archaeological Society of Finland,
22 Saarijärvi, pp. 176–211
- 23 Márquez B, Baquedano E, Pérez-González A, Arsuaga JL (2016) Microwear analysis of Mousterian
24 quartz tools from the Navalmaíllo Rock Shelter (Pinilla del Valle, Madrid, Spain). *Quat Int*.
25 <https://doi.org/10.1016/j.quaint.2015.08.052>
- 26 Moss EH (1983) The functional analysis of flint implements. Pincevent and Pont d'Ambon: two case
27 studies from the French Final Palaeolithic. *BAR International Series* 177. Archaeopress, Oxford
- 28 Moss EH, Newcomer MH (1982) Reconstruction of Tool Use at Pincevent: Microwear and
29 Experiments. In: *Tailler! Pourquoi faire: Préhistoire et technologie lithique II, Recent Progress in*
30 *Microwear Studies*. *Studia Praehistorica Belgica Leuven* 2: 289–312
- 31 Mourre V (1996) Les industries en quartz au Paléolithique. Terminologie, méthodologie et
32 technologie. *Paléo*. <https://doi.org/10.3406/pal.1996.1160>
- 33 Odell GH (1978) Préliminaires d'une analyse fonctionnelle des pointes microlithiques de
34 Bergumermeer (Pays-Bas). *Bulletin de la Société préhistorique française*.
35 <https://doi.org/10.3406/bspf.1978.4398>
- 36 Odell GH, Cowan F (1986) Experiments with Spears and Arrows on Animal Targets. *J Field Archaeol*.
37 <https://doi.org/10.2307/530220>
- 38 Ollé A, Pedernana A, Fernández-Marchena JL, Martin S, Borel A, Aranda V (2016) Microwear
39 features on vein quartz, rock crystal and quartzite: A study combining Optical Light and
40 Scanning Electron Microscopy. *Quat Int*. <https://doi.org/10.1016/j.quaint.2016.02.005>
- 41 Pargeter J (2013) Rock type variability and impact fracture formation: Working towards a more
42 robust macrofracture method. *J Archaeol Sci*. <https://doi.org/10.1016/j.jas.2013.05.021>
- 43 Pargeter J (2011) Assessing the macrofracture method for identifying Stone Age hunting weaponry. *J*
44 *Archaeol Sci*. <https://doi.org/10.1016/j.jas.2011.04.018>
- 45 Pargeter J, Shea J, Utting B (2016) Quartz backed tools as arrowheads and hand-cast spearheads:
46 Hunting experiments and macro-fracture analysis. *J Archaeol Sci*.
47 <https://doi.org/10.1016/j.jas.2016.08.001>
- 48 Plisson H, Beyries S (1998) Pointes ou outils triangulaires ? Données fonctionnelles dans le
49 Moustérien levantain [suivi des] Commentaires de J. Shea, A. Marks, J-M Geneste et de la
50 réponse des auteurs. *Paléorient*. <https://doi.org/10.3406/paleo.1998.4666>
- 51 Rankama T (2002) Analyses of the quartz assemblages of houses 34 and 35 at Kauvonkangas in

- 1 Tervola. In: Ranta H (ed) Huts and Houses. Stone Age and Early Metal Age Buildings in Finland.
2 National Board of Antiquities, Helsinki, pp 79–108
- 3 Rodríguez-Rellán C (2016) Variability of the rebound hardness as a proxy for detecting the levels of
4 continuity and isotropy in archaeological quartz. *Quat Int.*
5 <https://doi.org/10.1016/j.quaint.2015.12.085>
- 6 Rots V (2016) Projectiles and hafting technology. In: Iovita R, Sano K (eds) *Multidisciplinary
7 Approaches to the Study of Stone Age Weaponry*. Springer, Dordrecht, pp 167–185
- 8 Rots V, Lentfer C, Schmid VC, Porraz G, Conard NJ (2017) Pressure flaking to serrate bifacial points
9 for the hunt during the MIS5 at Sibudu Cave (South Africa). *PLoS ONE*.
10 <https://doi.org/10.1371/journal.pone.0175151>
- 11 Rots V, Plisson H (2014) Projectiles and the abuse of the use-wear method in a search for impact. *J
12 Archaeol Sci.* <https://doi.org/10.1016/j.jas.2013.10.027>
- 13 Seppä J (1995) *Poikkiteräisten kvartsinuolenkärkien tehokkuus: kokeellinen tutkimus*. University of
14 Helsinki
- 15 Siiriäinen A (1981) Problems of the East Fennoscandian Mesolithic. *Finskt Museum 1977*: 5–31
- 16 Taipale N (2012) *Micro vs. Macro. A microwear analysis of quartz artefacts from two Finnish Late
17 Mesolithic assemblages with comments on the earlier macrowear results, wear preservation
18 and tool blank selection*. MA dissertation, Uppsala University/University of Helsinki
- 19 Taipale N, Knutsson K, Knutsson H (2014) Unmodified quartz flake fragments as cognitive tool
20 categories: testing the wear preservation, previous low magnification use-wear results and
21 criteria for tool blank selection in two Late Mesolithic quartz assemblages from Finland. In:
22 Marreiros J, Bicho N, Gibaja Bao J (eds) *International Conference on Use-Wear Analysis: Use-
23 Wear 2012*. Cambridge Scholars Publishing, Newcastle upon Tyne, pp 352–361
- 24 Tallavaara M, Manninen MA, Hertell E, Rankama T (2010) How flakes shatter: A critical evaluation of
25 quartz fracture analysis. *J Archaeol Sci.* <https://doi.org/10.1016/j.jas.2010.05.005>
- 26 Tardy N, Vosges J, Varoutsikos B (2016) Micro-blade production on hyaline quartz during the Late
27 Neolithic of northern Greece (5400–4600 cal. B.C.): Examples from Dikili Tash and
28 Promachonas-Topolnica. *Quat Int.* <https://doi.org/10.1016/j.quaint.2015.11.139>
- 29 Tomasso S, Rots V, Perdaens Y, Crombé P, Meylemans E (2015) Hunting with trapezes at Bazel-Sluis:
30 the results of a functional analysis. *Notae Praehistoricae 35*: 239–251